Charles University

Faculty of Mathematics and Physics

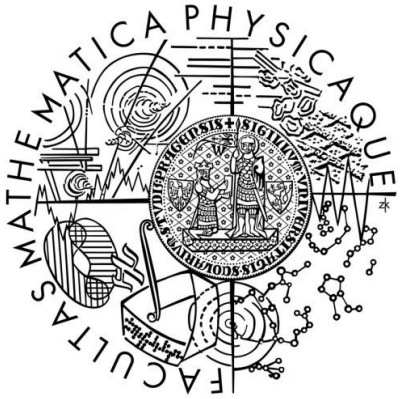

HABILITATION THESIS

Mgr. Mykhailo Vorokhta, Ph.D.

Understanding the Surface Processes at a Gas-Solid Interface by Near-Ambient Pressure XPS

Prague 2022

Acknowledgments

As the specifics of experimental work in surface science usually implies teamwork, most of the results presented here were obtained by cooperating with different researchers. I want to thank those people, as this thesis would never have appeared without them. I thank prof. Vladimír Matolín and prof. Iva Matolínová for letting me join the Nanomaterials Group and for all the help and support they always provided for me. Then, I would like to thank all my other colleagues from the Department of Surface and Plasma Science at Charles University, with a special mention of my friend doc. Ivan Khalakhan and Ph.D. students Lesia Piliai and Thu Ngan Dinhová.

I also want to express my gratitude to scientists from different foreign institutions for fruitful collaborations and discussions that resulted in numerous publications forming the basis of this thesis, especially dr. Oleksii Bezkrovnyi, prof. Martin Vrňata, and prof. Jose Rodriguez.

Last but not least, my greatest thanks go to my family and friends for their constant support and motivation.

Contents

Appendices – Selected publications

1. Introduction

This Habilitation Thesis comprises my research conducted over the last 6 years since a new laboratory for *in-situ/operando* studies was built at the Department of Surface and Plasma Science of Charles University. The primary experimental technique in this laboratory is Near-Ambient Pressure X-ray Photoelectron Spectroscopy (NAP-XPS) which allows the chemical analysis of the surface of solid material, in the presence of a gas or vapor, at pressures in the mbar range. Information on the chemical state of surface atoms and the presence of adsorbate during exposure to gases is crucial in the field of heterogeneous catalysis in order to understand mechanisms of chemical reactions and to optimize the composition of catalysts. Other areas where NAP-XPS can be applied include studying gas sensing mechanisms of gas sensors and analysis of wet biological samples, or samples immersed in an electrolyte with an applied potential. The last is essential for studying the electrochemical degradation and corrosion of different materials for fuel cell and battery applications.

The sphere of my scientific interests has covered studies of a broad range of materials related to various fields of science. This is mainly due to the specifics of the work in our laboratory, which is part of the Large Research Infrastructure SPL-MSB (Surface Physics Laboratory - Materials Science Beamline) operating within the European CERIC-ERIC infrastructure. This provides open access for external users from all over the world. Hence, I have always tried to divide my research into what I consider "general research" and "my science". In one case, I participated in or performed measurements for different users and colleagues and often helped process the data and prepare a manuscript. In the second case, I conducted independent research with my own ideas and visions. This work was related to studies of surface phenomena on solid catalysts and chemiresistive gas sensors under operational conditions and is the basis of this Habilitation Thesis.

The thesis is written as a compilation of my selected 12 publications. The publications are presented as Appendices A1-A12 after a commentary providing general information on the problems studied, the techniques used, and briefly describing the results and their importance. In all these publications, my scientific contribution was pivotal or substantial in order to justify their inclusion in this thesis. Publications A1, A2, A5, A6, and A9-A12 are combined into a section containing the results from the *in-situ* study of different important industrial chemical reactions taking place on the surface of ceria-based catalysts. At the same time, papers A3, A4, A7, and A8 form a second section describing the *in-situ* NAP-XPS investigation of gas sensing mechanisms of different types of gas sensors.

I had a chance to work with scientists from the Brookhaven National Institute, the Advanced Light Source in Berkley, Elettra Synchrotron in Trieste, the Institute of Low Temperatures and Structure Research of the Polish Academy of Sciences, the Institute of Physics of the Czech Academy of Sciences, and the University of Chemistry and Technology, Prague. Thus, the articles presented in the thesis also contain experimental results obtained by my colleagues using Scanning Tunneling Microscopy (STM), Diffuse Reflectance Infrared Fourier Transform Spectroscopy (DRIFTS), Scanning Transmission Microscopy (TEM), Raman spectroscopy, catalyst activity measurements, sensor response measurements, and Density Functional Theory (DFT) calculations. However, the primary experimental technique used for investigations in all cases was NAP-XPS, operated by me, and providing the most important results. In some works, I also used synchrotron-based NAP-XPS and Synchrotron Radiation Photoelectron Spectroscopy (SRPES) in an Ultra-High Vacuum (UHV).

2. Physicochemical processes at a gas-solid interface

The exposure of a solid material to a gas leads to different surface processes at the gas-solid interfaces, which are determined by the interaction of surface atoms with the colliding particles (atoms or molecules). In simple consideration, the gas-solid surface interaction depends on several interconnected parameters such as the effective potential of the surface, the time of stay of the gas particles at this potential, and gas and surface temperatures [1]. The gas particles, for example, some molecules that collide with the solid surface, mostly end up in two final states: they can be scattered off or adsorbed on. In some cases, the atoms can be embedded into the surface, but this only happens when bombarding the surface with high-energy particles. Molecules are considered elastically scattered if they stay at the surface for a short time that is insufficient to dissipate their energy. As the dissipation of excess energy of molecules proceeds via energy exchange with the vibrating surface atoms, this time should be shorter than the period of vibration of atoms in molecules and solid materials ($\tau < 10^{-13}$ s). If so, they feel only the repulsive part of the surface potential. Only the momentum exchange between the gas molecules and surface atoms is experienced, resulting in their elastic (mirror) scattering. Molecules that stay on the surface for 10^{-13} s $< \tau < 10^{-12}$ s usually lose a small amount of kinetic energy and become inelastically scattered. Finally, the molecules that spend a long time ($\tau \geq 10^{-12}$ s) on a solid surface typically lose a substantial amount of energy and are considered to be adsorbed [2,3].

Depending on the type of interaction between the adsorbed particles and surface atoms, the adsorption of gases on solids is generally divided into physisorption and chemisorption. Physisorption takes place at temperatures close to the condensation temperature of the gas and originates from weak electrostatic and Van der Waals interactions, the bonding energy of which does not exceed 0.5 eV. At the same time, chemisorption implies the creation of a strong chemical bond between the adsorbed particles and the surface atoms with energy of several eV [4]. Specific points on a solid material surface where gas molecules adsorb are called adsorption sites.

Adsorption is a vital surface process in many physical and chemical systems and has many applications. It is used in different gas-purification and separation processes, such as capturing carbon dioxide and volatile organic compounds (VOCs) from industrial gas emissions [5] or the separation of noble gases [6]. It is also frequently used for determining the surface area of different porous materials [7]. Finally, gas adsorption, especially chemisorption, is a crucial step in heterogeneous catalysis [8] and determines the properties of gas sensors [9], two research areas on which this thesis focuses.

Other essential surface processes that occur at a gas-solid interface are diffusion and dissociation of the adsorbed molecules. In the case of weak interactions of the adsorbed molecules with the surface, or when their oscillating energy is high enough, the molecules are mobile and can jump between different adsorption sites on the surface. This process, called surface diffusion, depends on the surface temperature and height (activation energies) of the barriers the molecules must overcome to diffuse [10]. Surface diffusion competes with molecular desorption, which is the process of particles leaving the surface. Finally, molecular dissociation on a solid surface occurs when there is a strong chemical interaction between the adsorbed molecules and surface atoms. In many cases, this interaction weakens a chemical bond between atoms in the molecule so that it can be broken at a temperature substantially lower than when the molecule is in the free state [11].

2.1. Heterogeneous catalysis

Heterogeneous catalysis is a type of catalysis in which the phase of the catalyst is different from the phases of the reactants and products and is the basis of many chemical and energy conversion processes in the industry [11,12]. In this type of catalysis, the chemical processes – reactions typically occur at the solid-gas or solid-liquid interface. The function of a catalyst is to direct a chemical reaction through the most kinetically favorable pathway. The pathway of a given chemical reaction occurring on the surface of a solid catalyst usually includes several steps and processes with activation barriers. These processes may include adsorption and dissociation of adsorbed molecules (reactants), formation of different intermediate species, and formation and desorption of the reaction products [13]. All these processes occur at specific places on the catalyst surface, called active catalytic sites. Often, these comprise surface defects, step edges, atomic raws, and corners, all containing low-coordinated atoms with higher reactivity than those at so-called low-indexed (flat) surfaces [14]. The role of a suitable catalyst is to decrease the activation barriers (energies) of "useful" processes, thus helping to form desirable products at the end of the reaction (Figure 1) [13]. This ability of the catalyst determines its selectivity towards desirable reaction products. At the same time, the value by which these barriers are decreased usually determines catalyst activity. The catalyst activity depends on the nature of the material used and the concentration of the active catalytic sites on its surface [14]. The last is, in many cases, proportional to the surface area of the catalyst. As a result, it motivates the preparation of catalysts, mainly in the form of nanoparticles (NPs) dispersed on different supports [15]. The size of such NPs usually varies around 2-5 nm, providing them with a large surface area-to-volume ratio. This results in an increased number of specific adsorption/reaction sites on the surface of NPs and often provides the NPs with specific electronic

properties not present in bulk materials (so-called size effect) [16]. Also, in recent years, a new frontier appeared in heterogeneous catalysis where active metals in the form of single atoms are stabilized on supports [17,18]. Such catalysts are called single-atom catalysts and, in many cases, might represent the most efficient utilization of the active metal, which is very important in the case of preparing catalysts containing expensive noble metals.

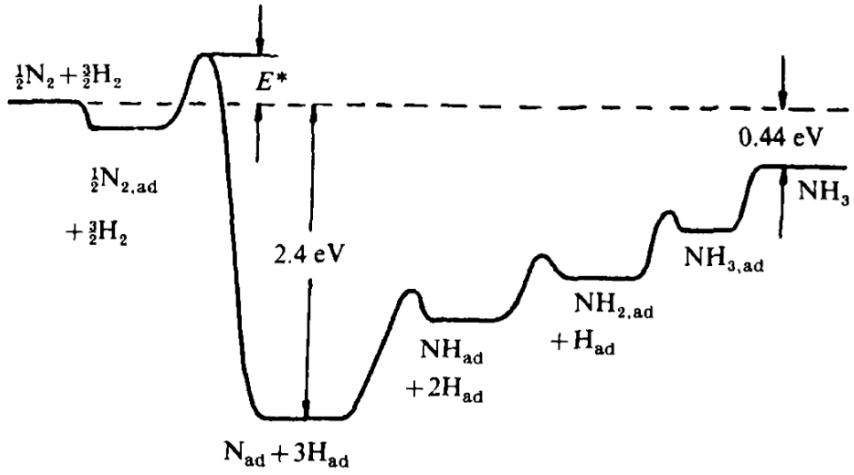

Figure 1. Potential energy diagram presenting the main intermediate steps in the synthesis of ammonia. Reproduced from [13]

Besides high catalytic activity and selectivity, every catalyst should possess another necessary characteristic: long-term stability under operational conditions. Fast catalyst deactivation would make even a very active catalyst impractical for applications. Catalyst deactivation is usually related to a decrease in active catalytic sites due to the sintering of small NPs into large particles or their coating with some inactive phase [19]. Both these deactivation mechanisms depend significantly on the interaction between the particles and the support. In the case of a weak interaction, the catalyst NPs easily sinter into large aggregates or detach from the support and are removed (washed) from the catalytic reactor. A very strong interaction might cause the migration of the material from the support onto supported NPs (so-called NPs encapsulation) [20,21]. Finally, other sources of undesirable phases that often deactivate catalysts are different reaction intermediates strongly bonding to and blocking active surface sites. Examples are CO poisoning and the formation of carbon coke in the case of different hydrocarbon conversion reactions on platinum-based catalysts [22].

As described above, catalyst activity, selectivity, and long-term stability are three essential parameters that should be increased when designing a suitable catalyst for a given catalytic reaction. The improved catalyst characteristics are typically achieved by optimizing its structure and composition [23]. At the beginning of catalyst research, a trial-and-error method was used to improve the properties of catalytic materials. By mixing different elements and compounds and testing them in a catalytic reactor, it was possible to design relatively active catalysts for many important chemical reactions. However, this approach was ineffective and required routine work, often based only on scientific intuition. The situation changed in the 1960s with the development of surface analysis techniques, and the first fundamental studies on the reactivity of different surfaces began to appear in surface science [24]. With the help of various techniques in surface analysis, such as Infrared Spectroscopy (IR) and X-ray Photoelectron Spectroscopy (XPS), it became possible to understand the reaction mechanisms of many important chemical reactions on different catalysts and to indicate routes for their improvement. The knowledge obtained allowed scientists to bring the design and optimization of catalyst structures to a completely different level.

2.1.1. Industrial heterogeneous catalysts

Real industrial heterogeneous catalysts are typically powders containing many different compounds. It might be a mixture of various metal oxides [25] or metallic NPs (1-10 nm) dispersed on porous supports with complex structures (Figure 2) [26,27]. The most widely used industrial oxide catalysts are aluminosilicates, which are used in the catalytic cracking of crude oil to produce different valuable hydrocarbons [28]. In the case of metal-based catalysts, cheap transitional metals are mainly used, such as Fe, Va, Ni, Co, Cu, etc. [27,29]. These metals are preferred catalysts for the production of ammonia (Harber process) [30] and different hydrocarbon transformations [31]. In some specific cases, noble metals such as Pt, Pd, Ir, Rh, or Au might be used as industrial catalysts [32]. However, due to their high price and low abundance in the earth's crust, they are only used in selective reactions where other metals show deficient activity or low electrochemical stability; low-temperature CO oxidation and H_2 dissociation [33,34], oxygen reduction reaction in proton-exchange membrane fuel cells [22,35], or oxygen evolution reaction in water electrolyzers [36,37].

Frequently used supports for metallic particles in industrial catalysts are SiO_2 and Al_2O_3 [38,39]. Their role is usually to ensure highly active metal dispersion and to protect them from agglomeration during the reaction. However, in many cases, the support actively participates in the chemical reaction and has an essential function in the reaction mechanism [40]. Especially reducible oxides such as TiO_2,

CeO_2, and Fe_2O_3 are frequently used as active supports for different metallic NPs [41–43]. Their activity is related to the fact that Ti, Ce, and Fe have multiple oxidation states and can switch between them by releasing or accepting surface oxygen atoms [44]. The support ability to release (reduce) and take back (reoxidize) oxygen is beneficial in many oxidative chemical reactions occurring via the so-called Mars-van-Krevelen reaction mechanism [45]. In addition, as described above, the catalyst support can strongly interact with the supported metallic NPs. The metal-support interaction (MSI) may modify the electronic structure of the supported NPs and, in turn, substantially change their catalytic properties [46]. The MSI, in many cases, results in synergistic effects between the support and active metal, leading to a substantial increase in the activity of the supported NPs [47,48]. It is also responsible for the stability of the whole catalytic system [20].

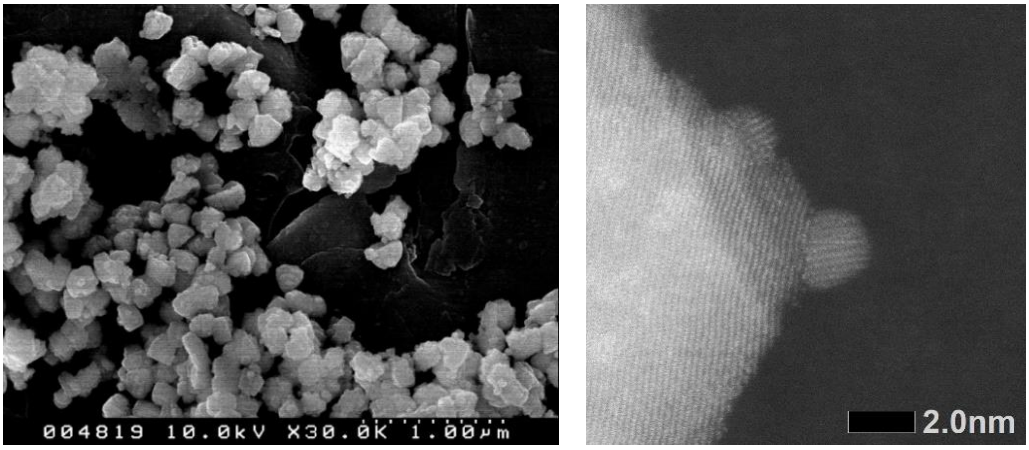

Figure 2. (a) Low-resolution scanning electron microscopy (SEM) image of a typical industrial catalyst (Pd/CeO_2); (b) high-resolution transmission electron microscopy (HRTEM) image of Ru metallic NPs supported by CeO_2.

Industrial catalysts are, in most cases, synthesized by wet chemical methods as a result of a chemical reaction in solution under certain conditions [49]. In most cases, nanostructured oxide supports are prepared by wet chemical approaches such as hydrothermal synthesis, template synthesis, self-assembly process, and hot-injection method [50,51]. At the same time, precipitation and impregnation are the most popular methods for depositing active metals onto the support [52]. In both cases, active metal is deposited from an inorganic salt solution. In the precipitation method, metallic NPs are precipitated onto the support surface by oversaturating the precursor solution. In some cases, the salt solution of active metal is mixed with the salt solution of the support, and they are precipitated simultaneously (so-called

co-precipitation). While in the case of impregnation, the synthesized support is impregnated by the precursor solution, and later the metallic NPs are formed by high-temperature heating. Besides popular wet chemical synthesis, other "dry" methods are sometimes used on a large scale for catalyst preparation. The preparation of a catalyst in the form of a thin film using different deposition techniques (magnetron sputtering, physical vapor deposition (PVD), chemical vapor deposition (CVD), atomic layer deposition (ALD), etc.) is one of the possible approaches [53].

2.1.2. Model catalysts

Industrial catalysts can be easily prepared and used in practice. However, it is often not easy to characterize and understand their functioning at a fundamental level due to their high complexity. Industrial catalysts are usually powders containing different crystallites with different surface facets exposed on the surface, each with its own surface reactivity [54,55]. Having such a complicated structure makes it very difficult to resolve the functionality of each component. Thus, the primary strategy in designing an effective catalyst is to exploit the model catalyst approach [56]. This approach includes studying simple systems and modeling the complex structures of a real catalyst. The large scale preparation of surfaces with defined crystal orientations and an examination of their ability to adsorb reactants and facilitate chemical reactions by various surface analysis techniques, may help to clarify the role of each component of the complex catalyst.

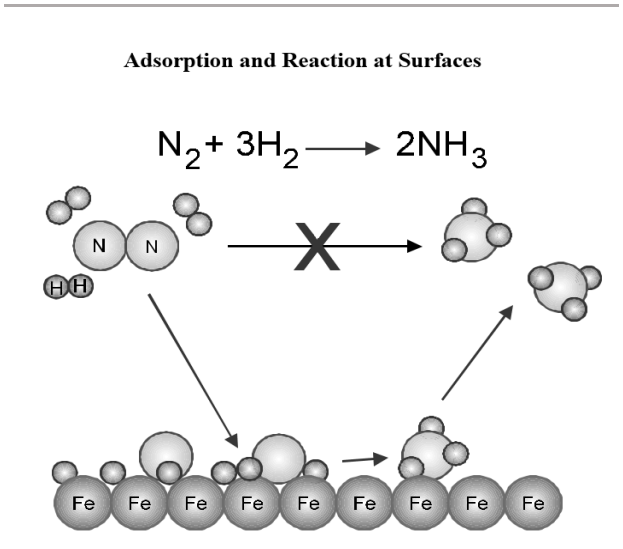

Figure 3. Synthesis of ammonia using Fe-based catalyst doped with alkali metals. Adapted from Ref. [57]

Single crystals represented the first simple models of well-defined surfaces that were prepared under the clean conditions of UHV. They provided a controlled method for the investigation of fundamental processes on catalyst surfaces [57,58]. The pioneering works by Ertl and Somorjai et al. [59–61] (Figure 3) are good examples of how fundamental studies of the reaction between nitrogen and hydrogen on different iron single crystalline surfaces resulted in a better understanding of ammonia synthesis. Many other essential reactions have been studied similarly on single crystals, giving deep insight into the fundamental processes of

molecule-surface interactions [62]. The relevance of such studies was demonstrated by the award of the Nobel prize in Chemistry in 2007, to Dr. Gerhard Ertl, for his studies of chemical processes on solid surfaces [63]. Later, to obtain a higher level of understanding and to bridge the so-called "materials gap" [64], more complex but still well-defined model systems, such as epitaxially grown metal oxide thin films, particles supported on oxide surfaces, or bimetallic surfaces have started to be studied [65,66] (Figure 4). Preparing such model systems made it possible to model the structure of many complicated real catalysts. By studying them, surface science has provided the framework to correlate the catalyst structure and composition with its activity in a given catalytic reaction. More information on the importance of studying model catalysts can be found in a special thematic issue, “Chemistry at surfaces”, edited by Hans-Peter Steinrück, Jörg Libuda, and David A. King and published in honor of Dr. Ertl [67], or other important reviews on this topic [16,68–71].

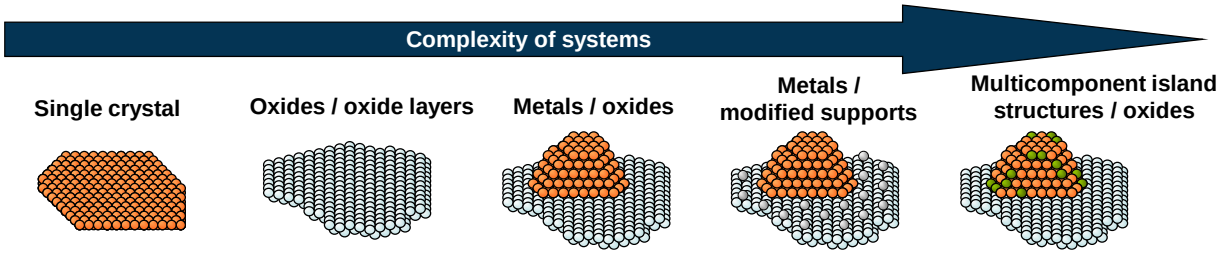

Figure 4. Controllable increase in the complexity of model catalysts. Adapted from Ref. [62].

2.1.3. *In-situ/operando* study in heterogeneous catalysis

Despite broadly studying different catalytic systems using traditional surface analysis techniques that primarily work under UHV conditions, the results usually explain only fundamental processes on catalyst surfaces. They often cannot explain what occurs on the surface of a catalyst under working conditions, and it is pivotal to investigate catalyst structure at the atomic level under reaction conditions. Such studies can help to understand the processes that take place on the catalyst surface, find a correlation between the catalyst structure and performance, and determine catalytic reaction mechanisms at the molecular level. The information can be later used to design catalysts with unique properties [72]. However, it is an essential and challenging task because the catalyst structure can change unpredictably along with changes in the pressure of reactants and the temperature of the catalyst, influencing, in turn, the reaction mechanism (Figure 5). Detailed investigations of structure-function-

based relationships in heterogeneous catalysts demonstrates that catalysts are not materials with static surface and bulk structures [73,74]. Rather, they are dynamic systems, the structure of which may change depending on the local reaction conditions, which may induce modifications of the chemical properties.

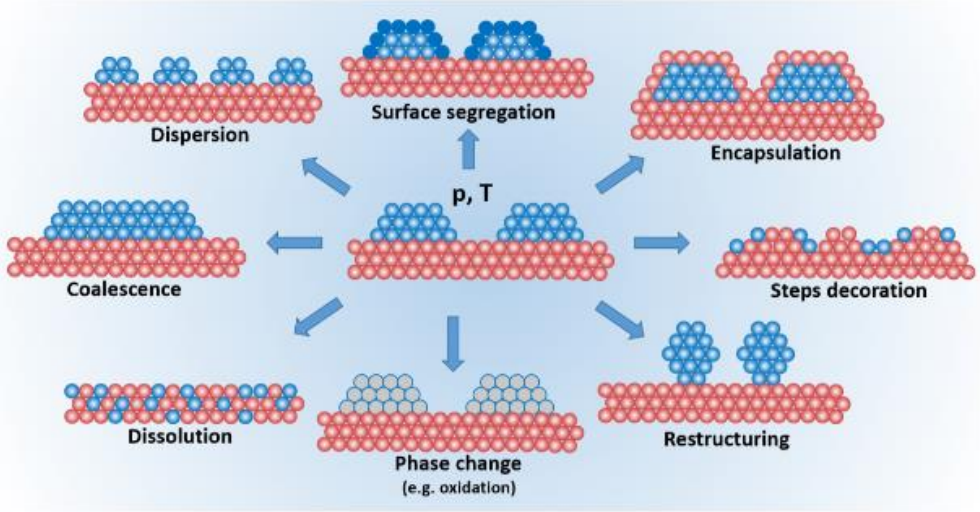

Figure 5. Examples of possible structural changes of a catalyst (metal NPs dispersed on an oxide support) exposed to a high-presure gaseous environment at a high temperature.

To pass the so-called "pressure gap" and investigate the processes on a catalyst surface at high gas pressures, the most popular approach is related to strategies for adapting standard analytical techniques, typically working in UHV for high-pressure measurements [72]. Indeed, many powerful analytical techniques used for characterizing catalysts, such as XPS, SEM, or TEM, generally work under UHV conditions. In that case, the catalyst can be characterized only *ex-situ* when the sample is exposed to air before each characterization. Air exposure, in many cases, initiates structural changes in the catalyst surface and introduces different contaminations. The possibility of analyzing a catalyst surface while exposing it to gases at high pressures and elevated temperatures, called an *in-situ* study, is thus vital [75]. The importance of the *in-situ* study is shown in Figure 6, displaying catalyst evolution during its lifetime. Performing *in-situ* investigations makes it possible to identify changes in catalyst structure and detect the intermediate species formed on its surface during each treatment and reaction [75,76].

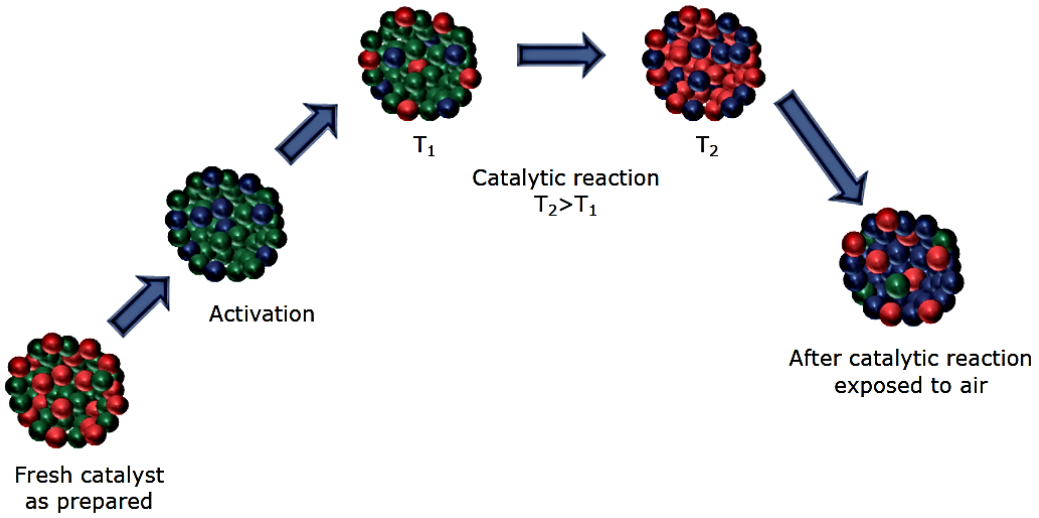

Figure 6. Catalytic evolution of an NP during its lifetime. Reproduced from Ref. [66]

In addition to the term *in-situ* study, another term often used in heterogeneous catalysis is the *operando* study, which was introduced into the catalysis literature relatively recently, in 2002 [77]. *Operando* is taken from Latin, which means "working" or "operating", i.e. gaining information from the "operating" sample. Generally, it means an *in-situ* study of the catalyst simultaneously with kinetic measurements of the catalytic reaction occurring on its surface. The last provides definitive evidence of the catalyst operation; thus, such an investigation can be considered to be performed under operationing conditions, i.e. *in-operando*.

In-situ/*operando* studies in heterogeneous catalysis are usually implemented through the development of various high-pressure cells (reactors) equipped with photon/electron transparent windows that allow the application of traditional spectroscopic and microscopic methods for the study of solid-gas interfaces. The most widely used *in-situ/operando* techniques in heterogeneous catalysis are NAP-XPS, high-pressure X-ray absorption spectroscopy (*in-situ* XAS), *operando* Raman and IR spectroscopies, high-pressure scanning tunneling microscopy (HP-STM), environmental SEM (E-SEM), and high-pressure or environmental TEM (E-TEM) [73,74,78,79]. Because each technique provides unique and complementary information on the catalyst state, several *in-situ/operando* methods are usually combined to identify dynamic changes in catalysts under operationing conditions [80] (Figure 7).

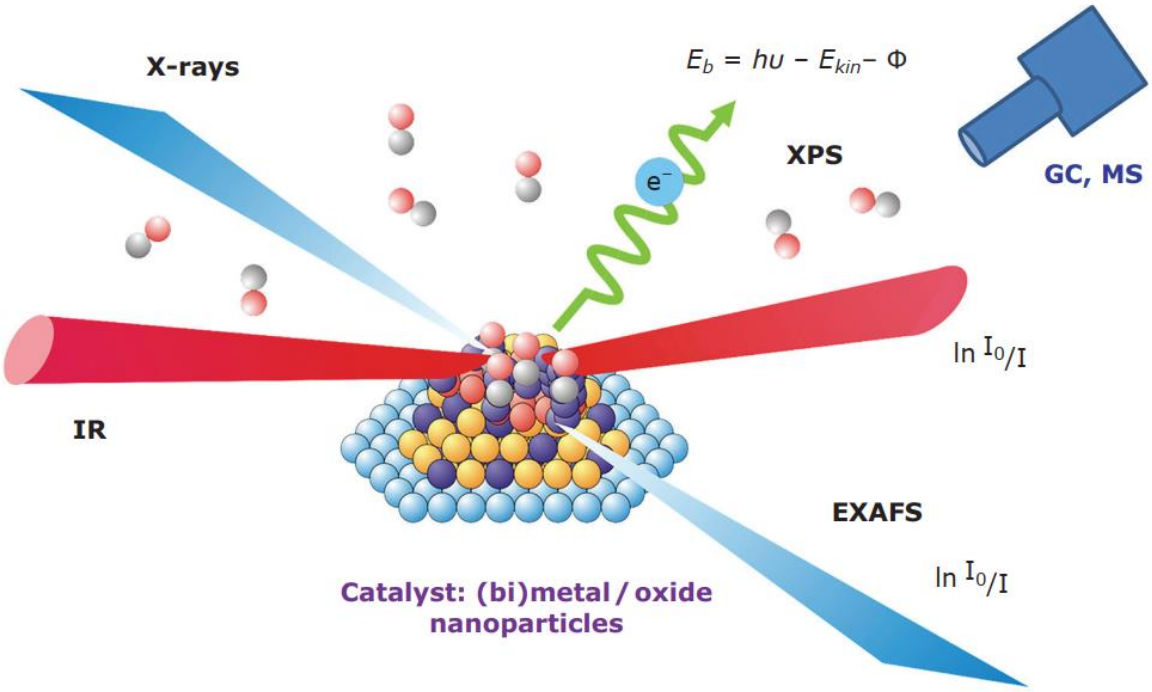

Figure 7. Combining several in-situ/operando techniques. Reproduced from Ref. [71]

2.2. Chemiresitive gas sensors

A chemiresistive gas sensor is a type of gas sensor that uses a chemiresistor as a sensing layer. Chemiresistors are materials, the electrical conductivity of which depends on the surrounding chemical environment [81]. Many different materials have chemiresistive properties. Among them are metal-oxide (MOX) semiconductors [82], conductive organic polymers and porphyrins [83], and various nanomaterials such as carbon nanotubes, graphene, and some NPs [84,85]. The sensing layer is usually deposited on a non-conductive platform containing an array of electrodes with small gaps (Figure 8). The electrodes are generally made of chemically resistive metals such as gold or platinum and should have good ohmic contact with the deposited film for measuring its electrical resistance.

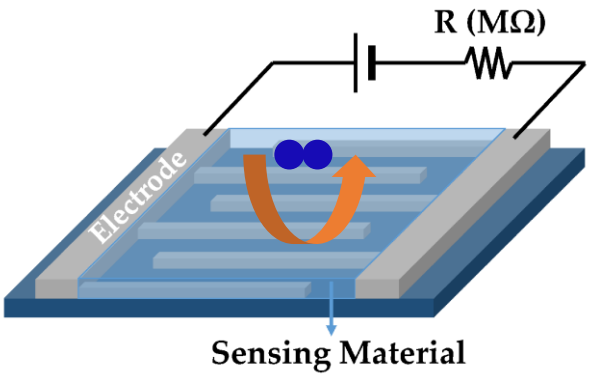

Figure 8. A basic scheme of a chemiresistive gas sensor. Reproduced from Ref. [76]

In the chemiresistive gas sensor, a direct chemical interaction occurs between the sensing material and the detecting analyte. The detectable gases either extract electrons from- or release them to- the sensitive layer, thus acting as electron acceptors or donors and modulating the electrophysical properties of the sensitive layer [82]. It initiates changes in layer resistance, signaling the presence of the detected analyte in the environment. In most cases, the changes in resistance are proportional to the concentration of the analyte, allowing its quantitative analysis. Thus, the performance of a chemiresistive gas sensor is usually described by a number of different parameters, such as sensitivity, selectivity, detection limit, response time, stability, and detection range [86]. All these parameters strongly depend on the type and structural properties of the chemiresistor and the surface processes occurring on its surface. The last include processes of adsorption-desorption of gases and surface catalytic reactions.

2.2.1. Metal-oxide semiconductor gas sensors

Metal-oxide (MOX) semiconductor gas sensors are the most widely known and used class of chemical sensors. They were first introduced in 1960s and originated from studying SnO_2 and ZnO thin

films, which were reported as promising materials for detecting inflammable gases [87,88]. MOX-based gas sensors have been commercialized since 1990 [89–91]. Despite commercialization, research on MOX-based sensors is still ongoing [92]. It has been accelerated especially since the recent development of nanomaterials and nanotechnologies. It was demonstrated that reducing grain size in the sensing layer to nanometer dimensions substantially improved its sensing properties [93]. In addition, the application of different low-dimensional MOX nanoobjects, such as nanowires (NWs), nanorods (NRs), nanosheets, and nanobelts, has recently been proposed for preparing susceptible chemosensitive layers [94].

Two main models are commonly used for describing the gas detection mechanism for MOX-based gas sensors: the ionosorption model and the oxygen vacancy model [95]. The key step in the ionosorption model (Figure 9) is the formation of charged oxygen species on the chemiresistor surface upon exposure to an oxygen-containing environment [96]. It is assumed that at low temperatures (≤ 473 K), chemisorbed oxygen molecules capture electrons from the MOX surface, forming superoxide molecules (O_2^-). With increasing temperature, they extract additional electrons and dissociate, creating a layer of chemisorbed O^- or even twice-charged O^{2-} ions. The extraction of free electrons from the conduction band of the chemiresistor, in general, is supposed to decrease the conductivity of an n-type semiconductor and increase a p-type one [96,97]. But more importantly, it leads to the formation of so-called space-charged regions at the surface, which, in the case of a nanostructured layer, work as potential barriers preventing the movement of the remaining free charge carriers (electrons in an n-type semiconductor and holes in a p-type one) in the layer. Adding a reducing gas to the exposure medium of the sensor leads to a catalytic reaction on the chemiresistor surface that lowers the concentration of chemisorbed oxygen species. This process brings electrons back to the surface and affects conductivity of the layer [98]. At the same time, a more oxidizing agent than oxygen in the atmosphere will increase the space-charge region causing the opposite changes in resistance of the layer.

The thickness of the space-charged region and, subsequently, the height of the potential barriers is determined by the concentration of the negatively charged oxygen species on the surface. It roughly equals the distance over which a local electric field created by these species influences the distribution of free charge carriers, i.e. the Debye length L_D :

$$L_D = (\varepsilon kT / 2\pi e^2 N)^{1/2}, \quad (1)$$

where T is the absolute temperature, ε is the material's dielectric constant, k is the Boltzmann constant, and N is the concentration of free charge carriers. For most MOX semiconductors, the Debye length usually stays in the nanometer range [99]. Thus, if a nanostructured MOX layer containing nanoobjects with the size d

that fulfills the relation $d < 2L_D$, the objects are fully involved in the space-charge layer. Consequently, such a layer is supposed to have significantly improved sensing properties compared to the bulk material.

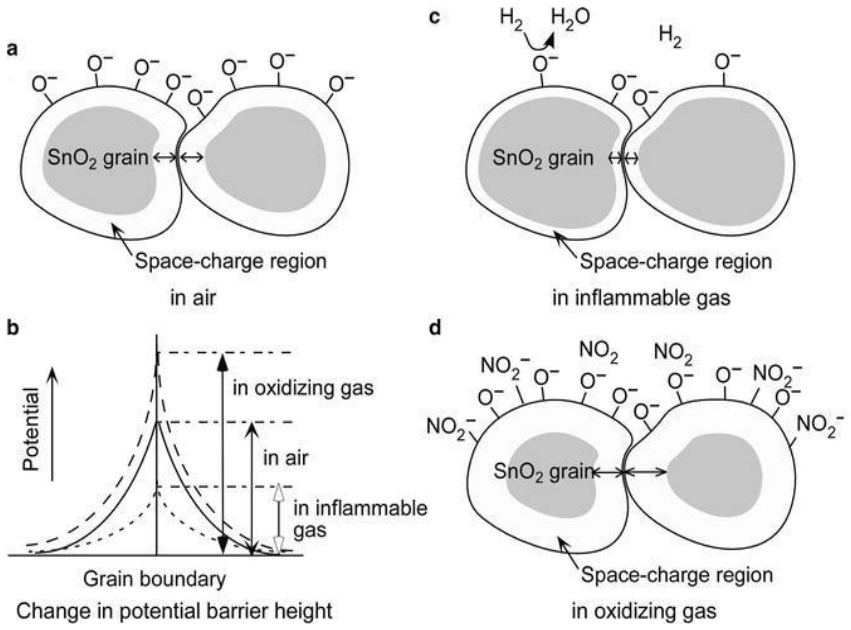

Figure 9. Ionosorption model describing the gas sensing mechanism of SnO_2-based gas sensor. Reproduced from Ref. [87].

The oxygen vacancy model is the second most popular model explaining the gas sensing mechanism of MOX-based sensors. Supporters of this model deny oxygen ionosorption and connect the sensor conductivity with the concentration of oxygen vacancies on the surface of the chemiresistor [95,100]. It is suggested that the exposure of the sensor to a reducing analyte increases the concentration of surface oxygen vacancies which, in turn, generates additional free charge carriers in the layer, causing the sensor response. At the same time, strongly oxidizing analytes such as NO_2, should have the opposite effect due to the process of filling oxygen vacancies. It should be noted that there are other less popular models for MOX-based sensor gas-sensing mechanisms that suggest considering analytes as direct electron donors or acceptors (the charge transfer mechanism) [101].

The existence of many different and sometimes even controversial mechanistic descriptions of the processes occurring on the surface of MOX-based gas sensors has motivated researchers to investigate them with the application of recently developed *in-situ/operando* surface analysis techniques [95,102]. The advantages of

in-situ/operando experiments are expected to provide new insights into the sensing mechanisms of different MOX-based gas sensors and help to design high-performance gas sensors. It was also a motivation for the sensory studies presented in the results chapter of this habilitation thesis.

2.2.2. Phthalocyanine-based gas sensors

Metal-phthalocyanines (MPcs) are organic frameworks that take the form of large two-dimensional molecules containing four isoindole units linked by nitrogen atoms to a central metal ion (Figure 10) [103] [104]. The physicochemical properties of MPcs depend very much on the valency of the hosting ion, which opens the possibility of their tuning for different applications [105]. Due to the presence of delocalized and weakly bonded π-electrons in MPcs, they may act as electron donors and behave as p-type semiconductors [106,107]. The typical MPc molecules are ZnPc, MnPc, CoPc, NiPc, CuPc, and PbPc, and are best known as standard colorants for automotive paints and printing inks [108], but they also have applications in solar cells, catalysts, and recently in gas sensors [109–111].

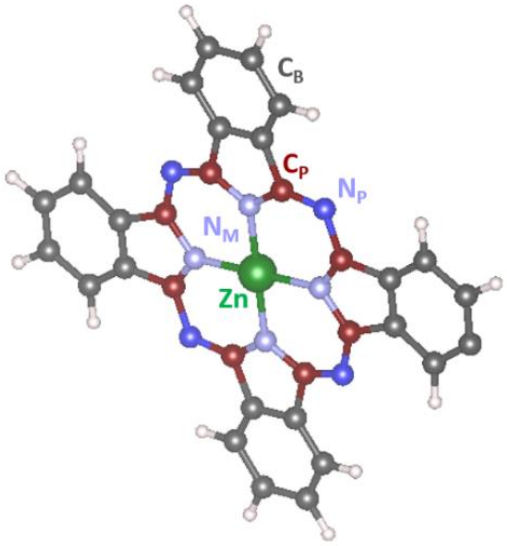

Figure 10. The schematic representation of the ZnPc molecule with the assignation of benzene-type and pyrrole-type carbons and different types of nitrogen atoms NP, NM.

In gas sensor applications, MPcs are mainly proposed to be used as very sensitive chemiresistors for detecting NO_2, making them promising candidates for detecting or monitoring this gas in real applications [112–117]. However, a few drawbacks of these materials must be mentioned, such as low reproducibility, extended response/recovery times, and short sensor lifetimes [118]. These problems are mainly connected with the strong-oxidizing effect that NO_2 typically demonstrates on organic compounds. It was found that massive NO_2 exposure may irreversibly change the MPcs layer [113]. Consequently, substantial efforts have been made recently to optimize working conditions and sensor operating procedures for protecting and maximizing its performance. This includes different methodologies focused on preventing sensor exposure to massive NO_2 doses and restoring its surface by external treatments, such as heating to a high temperature and laser irradiation [119].

The critical factor in improving NO_2 sensing parameters of MPcs-based gas sensors is a proper understanding of the NO_2 sensing mechanism of MPcs chemiresistors. Despite many studies, this is not fully understood at the molecular level [120]. Generally, it is assumed that the conductivity of MPcs is changed due to NO_2 binding to the central metal ion [121]. However, an alternative theory exists that relates the change in the conductivity to NO_2 binding to the pyrrole-type carbons and nitrogens [122]. The morphology of the chemosensitive layer and the presence of different defects also may drastically influence the sensing properties of MPcs chemiresistors [123].

3. X-ray photoelectron spectroscopy

Conventional XPS, also sometimes called Electron Spectroscopy for Chemical Analysis (ESCA), is a powerful and widely used method for the chemical analysis of solid surfaces. The technique was developed by Swedish physicist Kai Siegbahn in the 1960s and is based on the photoelectric effect [124]. This is the phenomenon of emitting electrons from an atom that is impinged by a high-energy photon. According to Einstein's Equation for the photoelectric effect, a photoelectron leaving the surface should have the following kinetic energy:

$$KE = h\nu - \varphi_s - BE \qquad (2)$$

where *KE*- electron kinetic energy, *BE* - electron binding energy, φ_s - work function of the surface. By measuring the kinetic energy of the ejected electron and knowing the photon energy and the surface work function, *BE* of the electron before ionization can be calculated. During XPS analysis, the situation is even easier because the analyzed sample is always in electrical contact with the spectrometer, and its Fermi level adjusts to the Fermi level of the spectrometer generating the additional surface potential. As a result, the surface work function of the sample becomes equal to the work function of the spectrometer φ_{spec}, which can be easily determined. So, the central Equation used for the calculation of *BE* of a photoelectron is as follows:

$$BE = h\nu - BE - \varphi_{spec} \qquad (3)$$

A schematic representation of sample analysis in a conventional XPS is shown in Figure 11. Here, a solid surface is irradiated with X-ray photons and ejects electrons, which are collected by an electron energy analyzer, thus producing an XPS spectrum. An XPS spectrum is a curve that shows the absolute number of photoelectrons detected at different *BE*s (usually presented in electron-volts (eV)). The XPS spectrum contains photoelectron peaks with *BE*s corresponding only to elements situated on the surface. Since each element from the periodic table of chemical elements has a unique electronic structure, comparing the measured peaks with the reference table data allows immediate identification of the surface element.

XPS is a surface-sensitive analytical technique that analyzes the surface up to several nanometers in depth. The probing depth of XPS depends directly on the kinetic energy of the photoelectrons generated, which, in turn, is determined by the X-ray photon energy [125]. Using standard laboratory X-ray sources with Al Kα or Mg Kα anodes that produce X-rays with energy above 1 keV, the probing depth

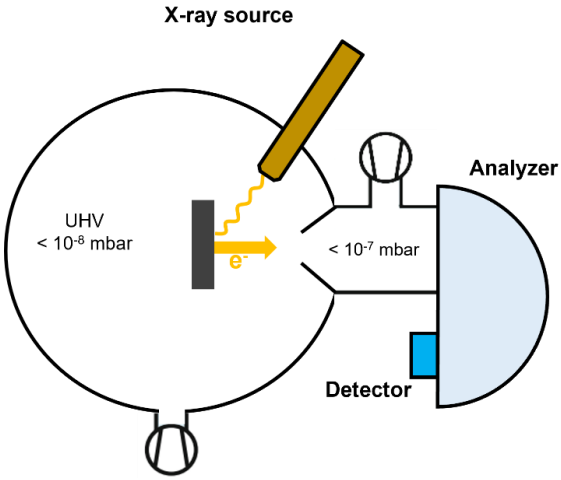

Figure 11. Schematic representation of a conventional XPS instrument.

varies from 3 to 6 nm, depending on the studied elements. For more surface-sensitive measurements, which might be necessary for different gas adsorption experiments, softer X-rays with energies below 1 eV must be used. In such cases, XPS measurement must be performed on a synchrotron, a special particle accelerator that can produce electromagnetic radiation in different energy ranges, including soft X-rays [126]. An additional advantage of synchrotron light is its very high intensity which might be critical for some XPS studies. Those XPS measurements that use synchrotron radiation are called SRPES measurements.

Examples of XPS spectra acquired from a solid surface using an X-ray source with an Al Kα anode that generates photons with an energy of 1486.6 eV are presented in Figure 12. The broad spectrum, called a survey spectrum, contains all photoelectron peaks that can be excited by X-ray on the studied surface (Figure 12a). The survey is usually measured with lower resolution and helps only identify what elements are on the surface. After that, the most intense characteristic peaks of these elements are collected separately with better resolution. Since the electronic structure of an atom is usually influenced by the chemical environment, the position of XPS peaks corresponding to this atom might be shifted by several eV, compared to the neutral state, if it chemically interacts with neighboring atoms and changes its oxidation state. This phenomenon is called chemical shift and is widely used in XPS analysis to identify different chemical compounds and interactions between atoms [127]. An example of various chemical shifts for four different carbon atoms in the C 1s spectrum recorded from a surface that contained molecules of ethyl-trifluoroacetate is shown in Figure 12b.

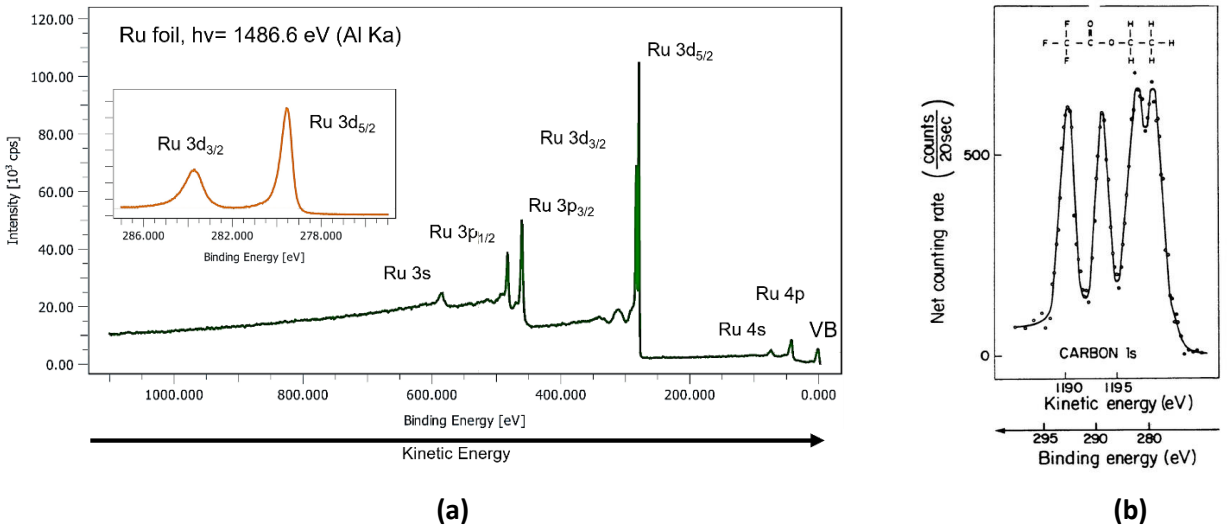

Figure 12. (a) XPS survey and Ru 3d spectra acquired from Ru foil; (b) XPS C 1s spectrum of ethyl-trifluoroacetate. Reproduced from [128].

In addition to information on the oxidation state of chemical elements on the surface, XPS can also provide quantitative information about their amount. The relative atomic concentration of elements on the surface can be determined from the intensity of the XPS peaks after normalization by the sensitivity factors (coefficients that include different technical parameters of a spectrometer and intrinsic properties of the elements) [124]. All this makes XPS an indispensable tool for studying heterogeneous catalysts. However, the drawback is that conventional XPS is generally performed under UHV because of the high voltages applied in typical X-ray sources and electron energy analyzers. It limits the use of conventional XPS just for the general characterization of catalyst composition and for studying the model catalyst surface reactivity after gas pre-adsorption [129]. The latter is usually done on a synchrotron, requiring a high-intensity soft X-ray source [47,130].

3.1. Near-ambient pressure XPS

At the early stage of developing XPS, it became clear that this method would be much more potent if it could also be used to study solid surfaces in gaseous environments. With XPS that can analyze a solid surface in the presence of gases, it becomes possible to *in-situ* investigate physical and chemical processes on the surface of catalysts and gas sensors [95,131]. Also, it can be used for analyzing strongly outgassing bio-samples, *in-situ* monitoring of growth process of a thin film, and for studying different oxidation/corrosion processes.

The scientists from prof. Siegbahn's group in Upsala were the first to work on improving the classical UHV XPS in the 1970s and made it possible to collect, for the first time, XPS spectra of gases and liquids [132]. They proposed to use differential pumping to separate places requiring a high vacuum (X-ray source and electron energy analyzer) from the sample zone containing a gas. Later on, this work was continued by Wyn Roberts [133], who constructed the first XPS spectrometer for investigating solid surfaces exposed to gases with pressures up to 1 mbar. In his work, the construction of XPS was improved by using a small high-pressure cell with an X-ray-transparent window (mostly SiN) and a differentially pumped electrostatic lens, features of a modern high-pressure XPS.

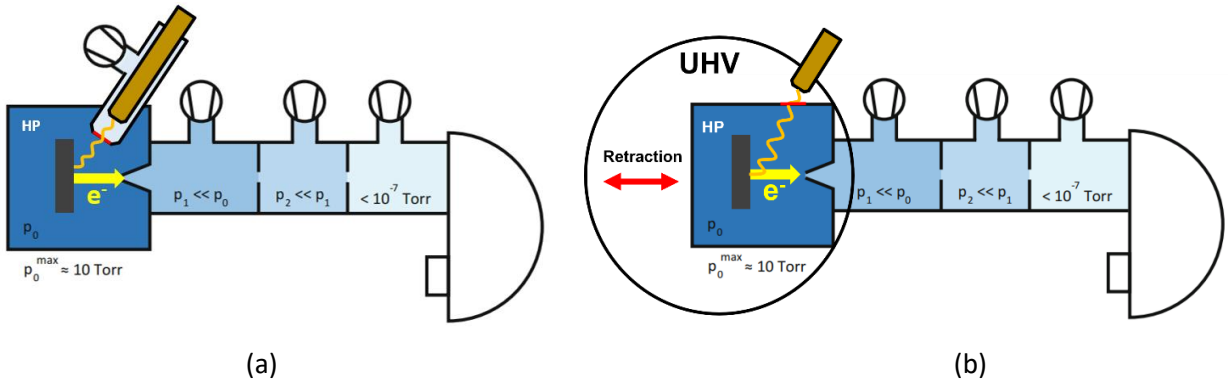

Figure 13. Different NAP-XPS configurations: (a) spectrometer with the backfilling chamber; (b) chamber-in-chamber design. Adapted from Ref. [124].

Nowadays, most high-pressure XPS spectrometers continue to work in the mbar range; therefore, the method is called NAP-XPS. They usually have one of two typical configurations [134]. The first, in which the whole analysis chamber is filled with gas during the measurement, is called NAP-XPS with a "backfilling" chamber (Figure 13a). Here, the X-ray source has its own pumping and is protected from gas by the SiN window. In the second case, the spectrometer is equipped with a small high-pressure cell (NAP cell) that is docked to the analyzer while doing high-pressure measurements and retracted from it if studying a sample under UHV conditions (Figure 13b). The advantage of the "backfilling" configuration is its lower price and relatively ample space in the analysis chamber for different modifications and

constructions. The NAP-XPS with NAP cell keeps the main UHV analysis chamber clean and offers a much broader research space for studying model catalyst surfaces prepared *in-situ*.

Modern NAP-XPS is typically equipped with a differentially pumped electron energy analyzer with several pumping stages, and collects electrons via a tiny nozzle with an entrance aperture smaller than 500 µm [135]. The small size of the nozzle aperture minimizes the gas flow and helps to reduce the pressure within the analyzer. For a better signal, the X-ray beam has to focus on a small area on the sample surface, precisely in front of the nozzle (Figure 14a). Ideally, the sample-nozzle distance (*z* in Figure 14a) should be as small as possible. However, it cannot be smaller than 2 nozzle aperture diameters to avoid the influence of pressure drop in front of the nozzle on the surface chemistry. It also explains why NAP-XPS cannot work under gas pressures above several mbar. Indeed, the most fundamental limitation is connected with the scattering of photoelectrons by gas [131]. The gas particles inelastically scatter the photoelectrons on their way to the analyzer. Together with the energy of the photoelectrons, *E*, and the type of gas particles, the main parameters influencing this process are gas pressure, *p*, and the distance between the sample and nozzle, *z*. By knowing these parameters, the attenuation of an XPS peak with signal intensity, I_0, obtained under UHV by gas can be calculated using the Beer-Lambert law:

$$\mathrm{I} = \mathrm{I}_{\mathrm{vac}} \exp^{\frac{-z\sigma(\mathrm{E})\mathrm{p}}{\mathrm{kT}}} \qquad (4)$$

where $\sigma(E)$ is the electron-scattering cross-section of gas at kinetic energy *E*, and *I* is the signal intensity measured in the presence of the gas [136]. It should be mentioned that instead of using $\sigma(E)$, the inelastic mean free path of photoelectrons in gas (IMFP), $\lambda(E)$, is often used when the XPS signal attenuation by gas is discussed. The following equation describes the relationship between $\sigma(E)$ and $\lambda(E)$:

$$\lambda\,(\mathrm{E}) = 4\mathrm{kT}/\mathrm{p}\sigma(\mathrm{E}) \qquad (5)$$

Equation (4) then can be written as:

$$\mathrm{I} = \mathrm{I}_{\mathrm{vac}} \exp^{\frac{-4z}{\lambda(\mathrm{E})}} \qquad (6)$$

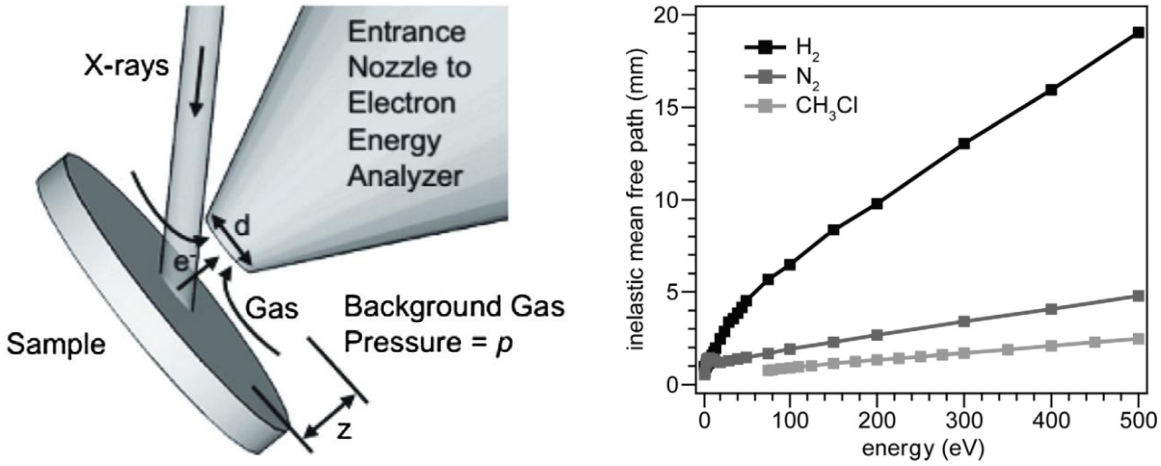

(a) (b)

Figure 14. (a) The sample environment during NAP-XPS experiment; (b) Experimentally measured inelastic mean free path of electrons in different gases. Adapted from Ref [125].

The IMFP of electrons in a gas strongly depends on the type of gas. Figure 14b presents an example of experimentally measured $\lambda(E)$ for 3 different gases (H_2, N_2, and CH_3Cl) with a pressure of 1 mbar at 300 K [135]. It can be seen that the IMFP of electrons with the typical XPS kinetic energies might be up to 20 mm for gases that consist of small molecules. However, it does not exceed several mm in the case of larger molecules. By applying these results to Equation 6, one can calculate that, for example, 90% of photoelectrons with an energy of 100 eV will be scattered by 1 mbar of N_2 at room temperature. Such a strong scattering already causes a significant loss of signal during the NAP-XPS study in gaseous environments with pressures in the mbar range. Further increases in gas pressure will result in an unacceptably low signal. Another factor that makes NAP-XPS impossible at gas pressures above several mbar is the decrease in X-ray flux due to absorption by the gas phase inside the analysis chamber.

Modern NAP-XPS facilities are mostly built in synchrotrons and are used to study surface chemistry at solid-vapor, solid-liquid, and liquid-vapor interfaces [137,138]. The reason for using synchrotron light is its high flux and the possibility of changing its energy, which is critical for surface-sensitive measurements. However, lab-based spectrometers that use conventional laboratory X-ray sources have started to be produced recently [139]. Although they are less powerful than the synchrotron-based ones, they offer much more space for research compared to the UHV XPS facilities. Besides providing general information on the chemical state of the surface atoms and the presence of different adsorbed species, NAP-XPS can

also be used to determine changes in the surface work function upon gas adsorption [140]. Also, in many cases, the presence of gas above the surface can help neutralize surface charging, which is a frequent problem in the XPS measurements of insulating samples. Thus, even though the studies are performed at several orders of magnitude lower pressures than in real applications, NAP-XPS is a compelling and desirable method for many scientists doing research on heterogeneous catalysis, gas sensors, electrochemistry, biotechnology, and other fields.`

3.2. NAP-XPS implementation in the Nanomaterials Group

A laboratory for combined *in-situ*/*operando* studies of gas/solid and liquid/solid interfaces has been set up recently in the Nanomaterials Group at the Department of Surface and Plasma Science (Figure 15). It contains unique equipment that was custom-built by SPECS GmbH (Berlin, Germany) and combines powerful surface analysis techniques, such as NAP-XPS and NAP-STM. It is also equipped with a specially designed electrochemical (EC) cell for performing electrochemical reactions on solid surfaces immersed in a liquid (electrolyte) and its subsequent surface characterization. All analytical techniques are connected via a two-floor system of UHV chambers and linear sample transfers, allowing sample movement for different measurements and treatments without a vacuum break.

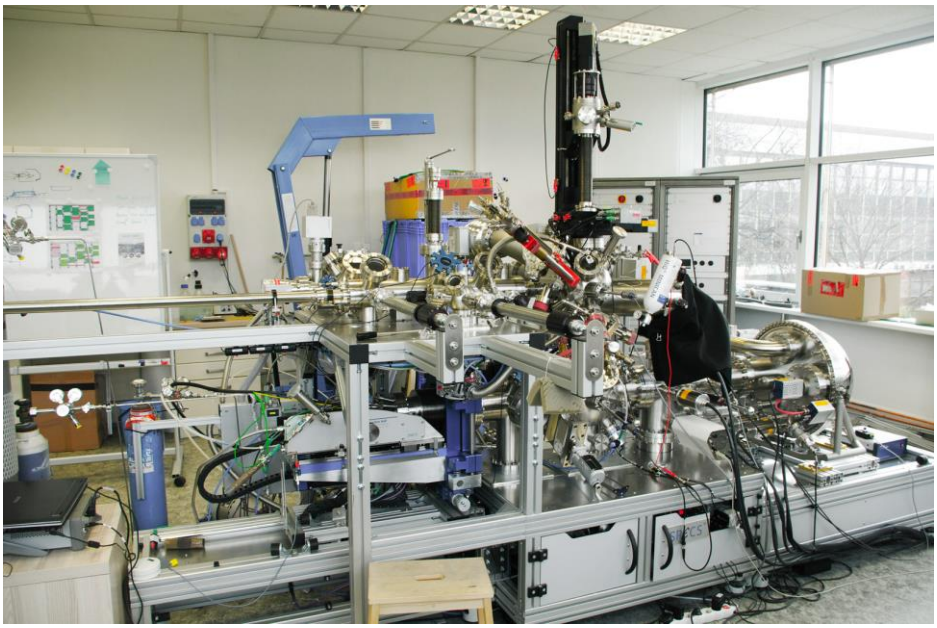

Figure 15. NAP-XPS and NAP-STM combined equipment at the Nanomaterials group.

The second floor of the equipment contains a so-called fast-entrance chamber for loading a sample onto the equipment and its evacuation. Then, the sample should be moved to the transfer chamber from which it can be sent for any type of analysis. On the second floor, there is also a UHV sample preparation chamber ($5x10^{-10}$ mbar) equipped with several electron-beam evaporators, an argon ion gun, a low-energy electron diffractometer (LEED), and a long UHV manipulator enabling heating of the sample to 1200 K and its movement to the first floor of the equipment for XPS or NAP-XPS analysis. The preparation chamber allows the *in-situ* preparation of well-defined model catalytic systems and different surface treatments of the *ex-situ* samples.

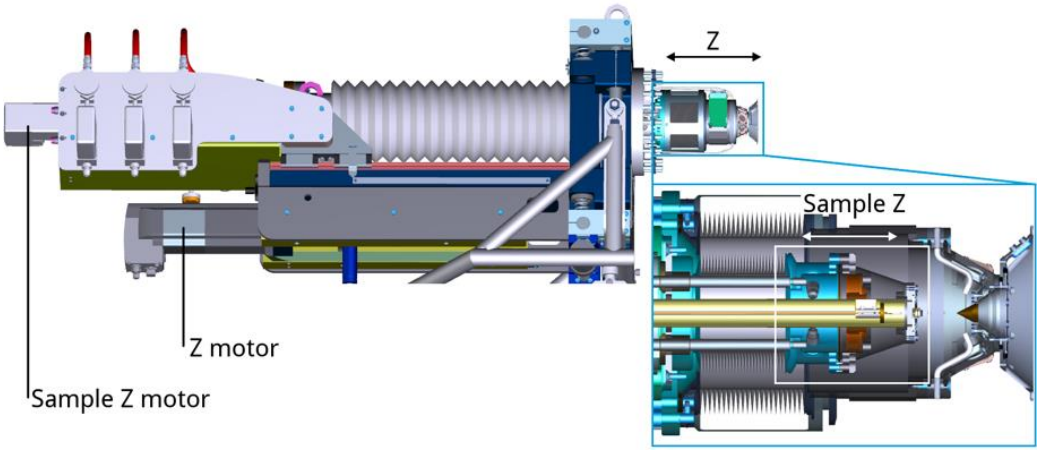

(a)

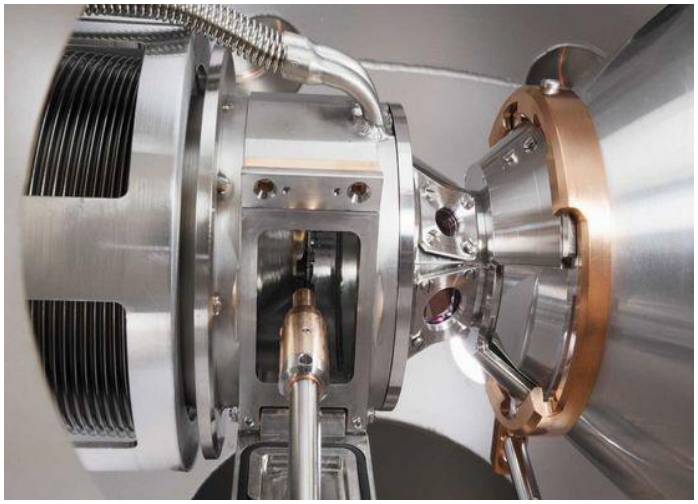

(b)

Figure 16. (a) DeviSim NAP manipulator with mounted NAP cell; (b) Inserting a sample into NAP cell.

The NAP-XPS part occupies the whole first floor of the equipment. It consists of the main analysis chamber ($1x10^{-9}$ mbar) separated from the sample preparation chamber by a gate valve. The analysis chamber is equipped with a focused monochromatized X-ray source of high intensity with an Al Kα anode (hν = 1486.6 eV), differentially pumped electron energy analyser (Phoibos 3500), and a NAP cell mounted on a special manipulator (NAP DeviSim) (Figure 16a). With the NAP cell manipulator, the cell can be approached and docked to the analyzer, evacuated, and filled with gases from 4 different inlets. During conventional UHV XPS analysis, the NAP cell is retracted from the analyzer, and the sample remains on the UHV manipulator. To perform a NAP-XPS measurement, the sample has to be taken from the UHV manipulator by a wobble stick, the UHV manipulator should be moved up, and the NAP cell has to be docked to the analyzer. After that, the sample can be inserted into the NAP cell via a special door (Figure 16b). The wobble stick is also used to close the door, after which the cell can be filled with gas or vapor. The maximum possible pressure during measurement is 5 mbar and during measurement, the sample should approach the nozzle at a distance of approximately 500 µm. The NAP manipulator also enables heating the sample inside the NAP cell to 773 K. The sample heating is done by contacting the hot sample stage heated by a beam of accelerated electrons from the rear (UHV) side.

4. Comments on articles

The results of this habilitation thesis are presented as a compilation of my 12 selected publications (denoted as **A1**-**A12**) related to investigating different surface processes and phenomena at the solid-gas interface. Topically they can be divided into two parts:

- *In-situ* study of chemical reactions on ceria-based catalysts.
- Understanding the gas sensing mechanism of chemiresistors.

However, this division does not always correspond to the chronological order of the publications in the appendices, as it was more important for me to preserve the logical course of work done.

The studies performed on different ceria-based catalysts continued the research that started long ago (approximately in 2007) in the Department of Surface and Plasma Science [141]. For almost 10 years, different ceria-based catalysts were prepared and investigated, mainly under UHV conditions, by researchers from the Nanomaterials group, to which I belong [47,142–144]. After building the new laboratory in 2015, allowing *in-situ*/*operando* investigations of catalysts, it was logical to continue that work but to use new and unique analytical techniques, which became available and, with considerable previous experience, allowed us to push our knowledge forward. I continued to investigate the model ceria-based catalysts prepared under UHV conditions (**A1**, **A2**, and **A12**), where it was possible to control the catalyst structure during preparation and, at the same time, to follow its evolution under reaction conditions. In parallel, fruitful cooperations were developed with scientists from the Institute of Low Temperatures and Structure Research of the Polish Academy of Sciences and the University of Lyon. They are experts in synthesizing different ceria-based powder catalysts and testing their catalytic activity. With mutual efforts, we have applied NAP-XPS to study various powder ceria-based catalysts and have obtained many valuable results (**A5**, **A6**, **A9**, and **A10**). In some cases, we combined studies on the model and real systems to better understand processes occurring on the catalyst surface (**A11**).

Besides studies on ceria-based catalysts, a new scientific direction based on the application of NAP-XPS to study sensitivity mechanisms of various gas sensors was established. The investigations were mainly carried out in collaboration with colleagues from the Institute of Physics of the Czech Academy of Sciences and the University of Chemistry and Technology Prague, experts in preparing and testing different chemiresistors. Notably, the investigation of the gas sensing mechanism with NAP-XPS was new and had never been reported in the literature previously. The results (**A3**, **A4**, **A7**, and **A8**) demonstrated the sustainability of our approach, which received good feedback from the sensor community in the form of scientific citations of our work.

4.1. *In-situ* study of chemical reactions on ceria-based catalysts

Cerium oxide (ceria) is a material with outstanding properties derived from the ability to quickly and expediently switch between Ce^{4+} and Ce^{3+} oxidation states, accompanied by the pronounced ability of the ceria surface to release and incorporate atomic oxygen [145]. In the oxide form of cerium, Ce^{4+} and Ce^{3+} oxidation states coexist (with the oxidized Ce^{4+} being the stable form), producing a redox couple responsible for high catalytic activity in different oxidative chemical reactions. Besides oxygen storage capacity, cerium oxide exhibits unique properties as a support for metal NPs that may significantly improve their catalytic performances [43,47,146]. These properties provide the basis for different ceria-based catalysts that may be tested on many important chemical reactions, including oxidation of CO and different hydrocarbons, water-gas shift reactions, the dry reforming of methane (DRM), and the conversion of methane directly into methanol. [31,147–149]. However, the structure and composition of ceria-based catalysts strongly influence their catalytic activity and selectivity. Different changes, such as nanofaceting, surface reconstruction and surface vacancy formation may appear on their surface under operational conditions, affecting their stability and catalytic performance [150–152].

4.1.1. Catalytic conversion of methane

[**A1**]

Liu, Z; Lustemberg, P; Gutiérrez, RA; Carey, JJ; Palomino, RM; Vorokhta, M; Grinter, DC; Ramírez, PJ; Matolín, V; Nolan, M; Ganduglia-Pirovano, V; Senanayake, SD; Rodriguez, JA. *In Situ Investigation of Methane Dry Reforming on Metal/Ceria(111) Surfaces: Metal–Support Interactions and C–H Bond Activation at Low Temperature*, Angew. Chem.-Int. Edit., 56 (42): 13041–13046, 2017.

[**A2**]

Lustemberg, PG; Palomino, RM; Gutiérrez, RA; Grinter, DC; Vorokhta, M; Liu, Z; Ramírez, PJ; Matolín, V; Ganduglia-Pirovano, MV; Senanayake, SD; Rodriguez, JA, *Direct Conversion of Methane to Methanol on Ni-Ceria Surfaces: Metal–Support Interactions and Water-Enabled Catalytic Conversion by Site Blocking*, J. Am. Chem. Soc., 140 (24): 7681–7687, 2018.

The work published in the **A1** article was completed during my 2-month stay in 2016 at the Brookhaven National Laboratory (BNL) in New York. After building the NAP-XPS laboratory in our department, we had little experience working with this equipment. Thus, I decided to visit a laboratory performing top-level research using the NAP-XPS technique and gain some experience in the *in-situ* study of catalysts. The laboratory of Dr. Jose Rodriguez, in the Chemistry Division of BNL, was a perfect option as they studied different ceria-based catalysts, which, at that moment, were of interest to us also. During

my stay, we mainly investigated different chemical reactions on the surface of model $M/CeO_2(111)$ (M: Ni, Co, Cu) catalysts using laboratory NAP-XPS. One reaction that we studied was DRM ($CH_4 + CO_2 = 2CO + 2H_2$), which is important in the large-scale production of hydrogen from natural gas. This was an extensive study on the activity of DRM catalysts, depending on the surface coverage of the admetals. Then, the reaction mechanisms for the most active samples were studied using NAP-XPS. Our study showed that the type of metal used was critical for DRM activity and system stability. Among all admetals, Co and Ni showed strong interactions with the support, adsorbing as ions with a 2+ oxidation state and demonstrated an outstanding result - room temperature activity for C-H bond dissociation. Reduction of the CeO_2 support at high temperatures under operational conditions of DRM stabilized Co and Ni in a metallic state. Such systems were also active in CH_4 activation and dry reforming, with Co/CeO_{2-x} being much more active than Ni/CeO_{2-x}. In the case of Cu, almost no DRM activity was observed and the Cu disappeared from the surface at high temperature due to evaporation. Our work showed that improved catalytic activity could be obtained by choosing the "right" metal-oxide combination and by controlling the effects of metal loading. The findings should help rationalize catalysts for reactions involving C-H bond dissociation.

The work published in article **A2** was partially carried out during my stay at BNL. However, the main results were obtained several months later in our joint experiment with Dr. Rodriguez during beamtime at the Advance Light Source (ALS) synchrotron in Berkeley, USA. Indeed, as the $M/CeO_2(111)$ (M: Ni, Co) catalysts already showed methane activation (cleavage of C-H bonds) at room temperature, we decided to study this phenomenon in detail, as it might be essential for the direct conversion of methane into methanol. The last is an important goal for the use of methane since methanol can be used as a starting chemical for the generation of different, more complex chemicals or as a fuel [153].

The reaction between methane and oxygen is typically performed for the direct conversion of methane into methanol, and there are two pathways for the reaction of methane with oxygen:

$$CH_4 + 1/2O_2 \rightarrow CH_3OH \qquad (7)$$

$$CH_4 + 1/2O_2 \rightarrow CO+H_2. \qquad (8)$$

From a thermodynamic point of view, the second reaction is more favorable at a temperature higher than 600 K. Thus, for obtaining methanol, the conversion should occur at temperatures below 500 K. In addition, it is crucial to partially oxidize the methane molecule by cleaving only one C-H bond and letting the remaining CH_3- radical interact with oxygen and hydrogen atoms (or directly with the OH group if

present). In work **A2**, we showed that Ni/CeO_2 is a promising catalyst for the direct conversion of methane into methanol. As in the case of DRM, it was demonstrated that the MSI between Ni and ceria makes possible the binding and activation of methane at low temperatures on the surface of the Ni/CeO_2 catalyst. The reaction of methane with oxygen in dry conditions proceeded via this pathway (8). However, adding water to the reaction chamber substantially increased selectivity toward methanol production. By applying NAP-XPS and DFT methods, we clarified the reaction mechanism and explained the effect of water. We showed that the Ni/CeO_2 catalyst also activated water at low temperatures; moreover, OH groups partially blocked active catalytic sites, preventing the complete dissociation of methane and enhancing selectivity towards methanol formation. The conceptual ideas presented in our work may be valuable in the design of other conventional metal/oxide catalysts that can transform methane into methanol.

4.1.2. Oxidation of CO on Au/CeO_2 and Au/$Ce_{1-x}Eu_xO_2$ catalysts

[**A5**]

Bezkrovnyi, OS; Vorokhta, M; Małecka, M; Mista, W; Kepinski, L. NAP-XPS study of $Eu^{3+} \rightarrow Eu^{2+}$ and $Ce^{4+} \rightarrow Ce^{3+}$ reduction in Au/$Ce_{0.8}Eu_{0.2}O_2$ catalyst. *Catalysis Communications*, 135, 105875, 2020.

[**A6**]

O. S. Bezkrovnyi, D. Blaumeiser, M. Vorokhta, P. Kraszkiewicz, M. Pawlyta, T. Bauer, J. Libuda, L. Kepinski. *NAP-XPS and In Situ DRIFTS of the Interaction of CO with Au Nanoparticles Supported by $Ce_{1-x}Eu_xO_2$ Nanocubes*, J. Phys. Chem. C, 124, 10, 5647-5656, 2020.

[**A11**]

Bezkrovnyi, O; Bruix, A; Blaumeiser, D; Piliai, L; Schötz, S; Bauer, T; Khalakhan, I; Skála, T; Matvija, P; Kraszkiewicz, P; Pawlyta, M; Vorokhta, M; Matolínová, I; Libuda, J; Neyman, KM; Kępiński, L. *Metal–support interaction and charge distribution in ceria-supported Au particles exposed to CO*. Chem. Mater., 34, 17, 7916–7936, 2022.

[**A12**]

L. Piliai, P. Matvija, T. N. Dinhová, I. Khalakhan, T. Skála, Z. Doležal, O. Bezkrovnyi, L. Kepinski, M. Vorokhta, I. Matolínová. *In-situ spectroscopy and microscopy insights into CO oxidation mechanism on Au/CeO_2(111) model catalyst*. ACS Appl. Mater. Interfaces. (*Accepted for publication in ACS Applied Materials & Interfaces, 2022*).

After my stay at BNL, I continued to study chemical reactions on ceria-based catalysts using NAP-XPS in Prague. From the beginning, my interests were focused mainly on CO oxidation on Au/CeO_2 catalysts. Since Haruta [154] showed that gold, finely dispersed on different oxides, might be an effective catalyst for the oxidation of CO at low temperatures, gold-based catalysts have been actively investigated,

with the aim of understanding the nature of their activities. Gold supported by ceria showed exceptionally high activity in CO oxidation [155,156]. At high temperatures, CO oxidation on Au/CeO_2 proceeded via the Mars-van Krevelen mechanism [157], describing it as consuming lattice oxygen from the support by CO molecules adsorbed on gold, with subsequent reoxidation of the ceria support by molecular oxygen. However, the situation was not simple at low temperatures, and recent publications indicate a debate on this problem [158]. Some relate the high activity of Au/CeO_2 for CO oxidation at low temperatures to the presence on the surface of different gold species, such as Au^+ or even negatively charged Au^- ions [159]. Others connect it with surface oxygen vacancies, which can accommodate weakly bonded molecular oxygen [160]. Finally, some works reported that high activities of Au/CeO_2 catalysts in low-temperature CO oxidation originated from the MSI between gold and the ceria support [161]. Modification of the ceria support with different dopings may have also significantly influenced its catalytic activity in CO oxidation, as it changed the catalyst reducibility [162].

To shed light on these questions, we performed a comprehensive *in-situ* study of different Au/CeO_2 catalysts. For this, a combinative approach was applied, which included an investigation of the powder-like and well-defined model Au/CeO_2 catalytic systems. The work was performed in fruitful collaboration with scientists from the catalysis group of prof. Kepinski, from the Institute of Low Temperatures and Structure Research of the Polish Academy of Sciences. From our group, the collaboration was initiated as a requirement for experts in synthesizing and testing powder-like catalysts. Prof. Kepinski's group was seeking specialists in surface science performing studies in surface chemistry. In several studies, we attempted to systematically investigate the influence of different parameters, such as doping the ceria support with other elements in order to fine-tune the MSI between gold and ceria, and the effect of surface ceria steps on the catalytic performance of Au/CeO_2 in CO oxidation.

In works **A5** and **A6**, we used NAP-XPS and DRIFTS techniques to investigate the effect of ceria doping by Eu on the reactivity of the $Au/Ce_{1-x}Eu_xO_2$ catalyst towards CO and its reducibility. It was generally expected that doping of ceria, consisting of tetravalent Ce^{4+} ions, with trivalent lanthanoids would increase the concentration of surface oxygen vacancies and positively influence catalyst activity in CO oxidation. However, the presence of the dopant also has a negative influence, and there is only an optimum concentration of about 20% Eu that positively influences the catalytic activity of Au/CeO_2 catalysts in CO oxidation [163]. Our study, performed on $Au/Ce_{0.8}Eu_{0.2}O_2$, showed that Eu-doping indeed increased the concentration of surface oxygen vacancies. But despite the higher concentration of vacancies, the doped catalyst was less reducible, substantially influencing its activity in CO oxidation. We

observed that the presence of Eu affected the MSI between gold and the support, manifesting in the formation of smaller concentrations of $Au^{\delta+}$ species on the surface of the doped catalyst. However, we concluded that the difference in the catalytic activity of Au/CeO_2 and $Au/Ce_{0.8}Eu_{0.2}O_2$ did not originate from an electronic effect of the Eu dopant on gold but rather from its impact on the size of the Au nanoparticles. Eu prevented the formation of the most active Au nanoparticles, which were present only on undoped ceria support.

Article **A11** presents an investigation of the MSI between Au NPs and $CeO_2(111)$ surface and its influence on reactivity towards CO. The primary motivation for this study was to shed light on the role and stability of different Au species in CO oxidation. In the literature, several highly reputable scientific groups have reported the existence and importance of negatively charged $Au^{\delta-}$ species on the ceria surface, seen primarily during *in-situ* investigations of CO oxidation on different powder-like Au/CeO_2 catalysts using infrared spectroscopy [159,164]. However, there have not been any reports on the detection of these species using XPS, which is a straightforward method for detecting chemical elements in different oxidation states. To investigate this problem in more detail, we performed a complementary study (NAP-XPS, SRPES, DRIFTS, and DFT calculations) of two different model Au/CeO_2 catalysts: a powder-like catalyst consisting of Au NPs supported by ceria octahedrons, preferentially with a $CeO_2(111)$ surface, and a flat epitaxially grown $CeO_2(111)$ surface supporting Au NPs. The study demonstrated the interplay between the charge distribution of Au NPs and the oxidation state of the ceria support, and how this influences the adsorption properties of CO molecules. It was found that on the stoichiometric $CeO_2(111)$ surface, the Au atoms from the Au NP/ceria interface were oxidized by oxygen atoms on the ceria surface into the Au^+ state, whereas all other Au atoms in the Au NP remained neutral (Au^0). Attempts to detect $Au^{\delta-}$ species on the stoichiometric $Au/CeO_2(111)$ surface were unsuccessful. In addition, DFT calculations performed on an $Au_{31}/CeO_2(111)$ model showed that no negatively charged Au species could be formed on such a catalyst.

Nevertheless, the calculation predicted that during partial reduction of the ceria support, some electrons could be transferred to Au NPs and delocalize among the neutral Au atoms of the metal particle, or form [$Au^{\delta-}$–O vacancy] complexes at the Au/ceria interface. This additional charge on Au NPs placed on the reduced ceria surface should have a clear spectroscopic signature in the form of a shift to lower BE of the Au 4f XPS spectrum. Thus, we performed an XPS investigation of the Au NPs deposited on a partially reduced ceria surface. The measurements indeed detected a slight shift of the metallic Au 4f doublet to a lower BE compared to the one measured on the stoichiometric $Au/CeO_2(111)$ catalyst. We also

investigated the behavior of the stoichiometric Au/CeO_2(111) surface upon exposure to CO at different temperatures. It was found that at temperatures above 200 °C, the ceria surface started to reduce, and this influenced the peak position of the Au 4f spectrum. The *in-situ* DRIFTS study of CO adsorption on the powder-like Au/CeO_2(111) sample showed that CO did not adsorb on the negatively charged $Au^{\delta-}$ sites, demonstrating its irrelevance for CO oxidation.

The model Au/CeO_2(111) system was further investigated in work **A12**. Here we studied the formative mechanisms of positive Au^+ species on the surface stoichiometric CeO_2(111) catalyst and their role in low-temperature CO oxidation. Some of the Au^+ ions were formed at the Au NP/ceria interface due to the MSI between gold and ceria. However, our work showed an additional mechanism for its formation connected with the density of ceria surface steps containing different peroxo species. *In-situ* NAP-XPS and NAP-STM investigation of the catalysts comprising high levels of positive Au^+ species under CO oxidation demonstrated elevated stability of Au^+ species in CO and its fast reduction under the reaction conditions of CO oxidation. This work also revealed that small Au NPs (below 2 nm) on the CeO_2(111) surface were unstable and relatively quickly grew into large particles above 5 nm. This growth occurred not via particle sintering but instead through the Ostwald ripening mechanism; i.e, the detachment of Au atoms from small Au NPs due to interactions with CO molecules and their reintegration into larger Au particles after desorption of CO_2 molecules.

4.1.3. Catalytic oxidation of CO on a Pt/CeO_2 catalyst

[**A9**]

Meunier, FC; Cardenas, L; Kaper, H; Šmíd, B; Vorokhta, M; Grosjean, R; Aubert, D; Dembélé, K; Lunkenbein, T. Synergy between Metallic and Oxidized Pt Sites Unravelled during Room Temperature CO Oxidation on Pt/Ceria. *Angew. Chem. Int. Ed.*, 60, 7, 3799–3805, 2021.

Besides studying CO oxidation on Au/CeO_2, I also investigated the mechanism of this reaction on a Pt/CeO_2 catalyst. This work was carried out in collaboration with Dr. Meunier from the University of Lyon. In the case of using Pt as the active metal in ceria-based catalysts, the main research interests were centered around the ability of the cerium dioxide support to accommodate Pt in an oxidized form, often described as the dispersion of Pt in the form of individual/single atoms [165]. In work **A9**, we studied active Pt species in the CO oxidation of a powder-like nanosized Pt/CeO_2 catalyst using NAP-XPS and DRIFTS. The results showed the presence of metallic and oxidized Pt during CO oxidation. However, we concluded that the presence of oxidized Pt species was not related to single Pt ions on the surface but

rather to the strong MSI of Pt NPs with the ceria surface. The mechanism of CO oxidation was described as the interaction between CO molecules adsorbed on the metallic Pt and oxygen supplied by PtO_x. Our work created a new perspective on the active nature of Pt catalysts, where both metallic and oxidic Pt phases can coexist.

4.1.4. Catalytic oxidation of propane on Ru/CeO_2 catalyst

[**A10**]

Bezkrovnyi, OS; Vorokhta, M; Pawlyta, M; Ptak, M; Piliai, L; Xie, X; Dinhová, T.H.; Matolínová, I; Kepinski, L. In-situ study of Ru/CeO_2 catalyst under propane oxidation. *J. Mater. Chem. A,* 10, 31, 16675-16684, 2022.

A Ru/CeO_2 catalyst typically shows promising activity in oxidizing CO, NO, and different hydrocarbons [166]. In the literature, it was generally related to the redispersion of Ru on the surface of ceria in the presence of oxygen at high temperatures [167]. However, our colleagues from prof. Kepinski's group noticed that Ru was relatively quickly deactivated after reduction pretreatment cycles, which generally should positively influence catalytic activity due to the creation of additional surface oxygen vacancies. To explain this deactivation, we completed an *in-situ* NAP-XPS investigation of the oxidation of propane (chosen as a model molecule) on a Ru/CeO_2 powder-like catalyst. The result of our study, presented in article **A10**, demonstrated for the first time that Ru/CeO_2 interaction with an oxygen-rich atmosphere at 573 – 773 K (300–500 °C) resulted in the oxidation of Ru to the Ru^{8+} state and its partial disappearance from the Ru/CeO_2 catalyst surface as volatile RuO_4. Moreover, we showed that Ru^{8+} in Ru/CeO_2 was unstable and was quickly reduced to Ru^{4+} after contact with air at room temperature, explaining why Ru^{8+} was not previously detected in catalysts studied mainly using *ex-situ* analytical techniques. Ru evaporation from the outer catalyst surface in the catalytic reactor allowed us to describe the mechanism of catalyst deactivation. In contrast, Ru evaporation and redeposition inside the powder well explained Ru redispersion on the ceria surface. It was also concluded that the mechanism of propane oxidation should include an interaction of propane molecules with the ceria surface coated with a thin layer of RuO_4, thus working as an effective oxidizer. This work became a clear example of the importance of *in-situ* studies in heterogeneous catalysis.

4.2. Understanding the gas-sensing mechanism of chemiresistors

The series of works dedicated to NAP-XPS studies of various chemiresistors was made in collaboration with colleagues from the Institute of Physics of the Czech Academy of Sciences and the University of Chemistry and Technology Prague. We were the first group to apply NAP-XPS in studies of gas sensors under operational conditions. For this, we developed a methodology that included XPS analysis of the sensor surface and measurements of its electrical resistance while controllably exposing it to different gases at high temperatures. The study was performed on several different chemiresistors. We started with SnO_2, which is an n-type semiconductor widely used as a sensitive layer for commercial chemiresistive gas sensors (**A3**). Our work then continued by studying CuO_x nanowires (NWs), ZnO nanorod (NRs)-based (**A4** and **A7**) and Zn-phthalocyanine-based (**A8**) gas sensors. The diverse materials researched were selected in an effort to demonstrate the universality of the method used.

4.2.1. *In-situ* NAP-XPS study of metal-oxide chemiresistors

[**A3**]

Vorokhta, M; Khalakhan, I; Vondráček, M; Tomeček, D; Vorokhta, M; Marešová, E; Nováková, J; Vlček, J; Fitl, P; Novotný, M; Hozák, P; Lančok, J; Vrňata, M; Matolínová, I; Matolín, V. Investigation of gas sensing mechanism of SnO_2 based chemiresistor using near ambient pressure XPS, *Surf. Sci.*, 677, 284–290, 2018.

[**A4**]

Hozák, P; Vorokhta, M; Khalakhan, I; Jarkovská, K; Cibulková, J; Fitl, P; Vlček, J; Fara, J; Tomeček, D; Novotný, M; Vorokhta, M; Lančok, J; Matolínová, I; Vrňata, M. New Insight into the Gas-Sensing Properties of CuO_x Nanowires by Near-Ambient Pressure XPS. *J. Phys. Chem. C*, 123, 49, 29739–29749, 2019.

[**A7**]

Piliai, L; Tomeček, D; Hruška, M; Khalakhan, I; Nováková, J; Fitl, P; Yatskiv, R; Grym, J; Vorokhta, M; Matolínová, I; Vrňata, M. New Insights towards High-Temperature Ethanol-Sensing Mechanism of ZnO-Based Chemiresistors. *Sensors*, 20, 19, 5602, 2020.

In work **A3**, an NAP-XPS investigation of chemical processes on the surface of a nanostructured SnO_2-based chemiresistor was carried out under various atmospheres (oxygen, argon, ethanol, oxygen/ethanol mixture) and at typical working temperatures of a MOX gas sensor (450 - 573 K). By following sensor resistance upon each exposure, we related chemical changes on the surface of the chemiresistor to its response to the analytes. Although we failed to observe oxygen chemisorbed on the oxide surface, the shift in XPS peaks, initiated by band-bending effects, indirectly confirmed it. This shift disappeared upon surface exposures to argon, oxygen/ethanol, and ethanol, indicating a decrease in the concentration of chemisorbed oxygen. We did not detect the formation of surface oxygen vacancies on

the sensor surface during exposure to an oxygen/ethanol mixture. However, different carbonaceous groups, such as ethoxy groups and acetaldehyde molecules, were observed. We concluded therefore that the results supported the existing theory regarding the mechanism of ethanol detection on SnO_2 sensors, as proposed by Kohl [168]. This relates sensor response to chemical reactions of ionosorped oxygen species with ethanol, leading to its oxidation.

After successfully applying NAP-XPS to study the ethanol-sensing mechanism of a SnO_2-based chemiresistor, we investigated a reducible oxide-based sensor to determine the role of surface oxygen vacancies in the detection of different gases by MOX-based sensors. In work **A4,** we focused on a CuO_x NWs-based gas sensor due to recent intensive studies of different nanostructured copper oxide layers for gas detection [169,170]. Our colleagues from the University of Chemistry and Technology Prague found that a gas sensor based on CuOx NWs had superior sensing properties for detecting both reducing (ethanol) and oxidizing (NO_2) gases. However, achieving its stable working parameters required a relatively long “warm up” procedure, including sensor exposure to a reducing atmosphere at elevated temperatures. The NAP-XPS investigation of the sensing properties of CuO_x showed that the as-synthesized CuO_x NWs consisted of a Cu_2O-based core coated with an approximately 10-nanometer-thick CuO layer. Such NWs can act as chemiresistors, but in the case of ethanol detection, they demonstrated an n-type "integral" response with poor detection parameters. However, after treatment in ethanol vapors at 450 K, the Cu_2O/CuO NWs switched to relatively stable Cu_2O NWs with a p-type response to ethanol, significantly improving detection parameters. It was found that during the detection of a low concentration of ethanol in an oxygen atmosphere at 400-450 K, the Cu_2O NWs were again coated with a CuO layer. However, the thickness of the surface CuO layer remained below 1 nm, not influencing sensor detection performance. The sensor exposure to strongly oxidizing NO_2 increased the CuO layer to about 2 nm, which also only slightly affected sensor performance. Our work revealed that for the Cu_2O/CuO-based sensor, the sensor response was driven not only by the exchange of electrons between the analyte molecule and the sensitive layer but also by different chemical changes in the chemiresistor layer.

In work **A7**, we applied the NAP-XPS technique to investigate ethanol and acetaldehyde sensing mechanisms of ZnO NRs-based chemiresistors by using the same measurement protocol as in the case of studying the SnO_2-based sensor. Our results revealed that the reaction of ethanol with ionosorped oxygen on the surface of ZnO NRs followed the acetaldehyde pathway. It was demonstrated that the acetaldehyde further decomposed the ZnO surface during the sensing process, leading to the accumulation of carbon, which decreased sensor performance. However, we proposed a new approach

for determining the sensor response to intense acetaldehyde exposures based on impedance measurements (so-called AC (alternating current) performance). It was shown that despite blocking oxygen chemisorption sites, the carbon contamination on the surface strongly affected the displacement component of the current, causing higher sensor responses in the AC mode. We also investigated the influence of water in the environment on the sensing performance of the ZnO NRs-based gas sensor, proving its high tolerance to humidity.

4.2.2. *In-situ* study of a Zn-phthalocyanine chemiresistor

[**A8**]

Tomeček, D.; Piliai, L.; Hruška, M.; Fitl, P.; Gadenne, V.; Vorokhta, M.; Matolínová, I.; Vrňata, M. Study of Photoregeneration of Zinc Phthalocyanine Chemiresistor after Exposure to Nitrogen Dioxide. *Chemosensors*, 9, 9, 237, 2021.

In work **A8**, we investigated the NO_2 sensing mechanisms of Zn-phthalocyanine (ZnPc)-based gas sensors and its regeneration by light-emitting diode (LED) illumination of various wavelengths (412–723 nm). By applying NAP-XPS, we showed that NO_2 molecules bound to the Zn atom in ZnPc, not only in the form of NO_2^- but also as NO^- formed after the partial decomposition of NO_2 on the surface. It was also found that NO_x species remained adsorbed on the ZnPc surface after the evacuation of gas from the system or its exposure to clean air. However, the illumination of the surface by the LED effectively stimulated the desorption of NO_X species. The regeneration efficiency of the light strongly depended on its wavelength and was the highest for 412 nm light, which promoted the desorption of more than 90% of NOx species after several seconds of illumination. The efficiency of photoregeneration was higher than that of typically used temperature regeneration.

The NAP-XPS study also showed that the oxygen released after NO_2 decomposition slowly oxidized the ZnPc layer, partially deactivating it. We demonstrated that the ZnPc-based sensor should be exposed to only very moderate doses of NO_2, since after overcoming defined NO_2 concentrations, it became irreversibly oxidized. In order to protect the sensor from complete deactivation during NO_2 detection, we developed a so-called "constant exposure dose" method for controllable sensor exposure to NO_2. It was demonstrated that this method, based on controlling the NO_2 exposure time, effectively ensured the sensor exposure to only a low dose of NO_2, causing a 10% change in the sensor resistance. In combination with LED photoregeneration, this revealed prospects for practical uses of ZnPc-based chemiresistors.

5. Conclusions

The main goal of this thesis was to demonstrate the importance of *in-situ/operando* investigations for understanding surface processes at a gas-solid interface. One of the most powerful analytical methods for such studies is NAP-XPS, which allows for direct chemical analysis of surfaces in the presence of gases. The introduction of NAP-XPS in the Nanomaterials Group enabled advanced scientific research in the fields of catalysis and gas sensors. This technique was applied for *in-situ* probing chemical reactions on various types of samples, starting from well-defined model surfaces up to real powder-like catalysts and operating gas sensors.

By studying ceria-based catalysts, it was demonstrated that they are dynamic entities that actively change after contact with gaseous reactants at high pressures, and often these changes can be caught only during *in-situ/operando* measurements. These can be chemical changes, as in the case of Co and Ni deposited on ceria (Appendices A1 and A2). These metal ions remain oxidized after catalyst preparation, but transform into the metallic state with increasing temperature under reaction conditions or morphological transformations, where tiny metal nanoparticles are transformed into large particles (Appendices A11 and A12) or redispersed on single atoms (Appendix A10). The results also shed light on the role of different gold species on undoped ceria (Appendices A11 and A12) and Eu-doped ceria (Appendices A5 and A6) surfaces in low-temperature CO oxidation reactions. Finally, the mechanisms of hydrocarbon oxidation and low-temperature CO oxidation were explained on Ru/CeO_2 (Appendix A10) and Pt/CeO_2 (Appendix A9) catalysts, respectively.

The NAP-XPS investigation of gas-sensing mechanisms of different chemiresistors demonstrated the success of this approach. Although it was impossible to detect oxygen ionosorption directly, the band-bending effects indirectly confirmed this process in the case of non-reducible MOX-based chemiresistors (Appendices A3 and A7). Combined with information on the chemical reaction proceeding on the sensor surface during the detection process, this brought additional experimental evidence for the ionsorption theory of gas sensing. By studying a reducible MOX-based gas sensor, such as a CuOx NWs-based one (Appendix A4), it was demonstrated that NAP-XPS analysis of the sensor surface provides direct information on MOX phases present on the surface during detection. This indicated that the response of a reducible MOX-based gas sensor might be determined not only by the change in concentration of the ionosorped oxygen on the chemiresistive layer but also by the chemical changes in it. Finally, investigating a ZnPc-based gas sensor (Appendix A8) showed that NAP-XPS might help explain the sensing and deactivation mechanisms of some vulnerable chemiresistors.

6. Outlook

A large part of this habilitation thesis is dedicated to studying different chemical reactions and catalysts that help to eliminate toxic emissions, such as CO or VOCs, into the atmosphere. However, this approach for fighting harmful emissions has disadvantages connected with the production of CO_2, causing environmental problems associated with global warming. It would be much better to transform the global economy and maximally decrease emissions in a way that directly depends on reducing fossil fuel consumption. For this approach, developing new materials that may be applicable to the production of clean energy from renewable resources is essential. The use of solar energy is one of the most promising substitutes for fossil fuels [171]. However, this requires the development of stable materials for efficient solar cells. Besides the established silicon-based materials, perovskite materials have recently been described that may have new applications in solar cells [172]. The only drawback in their large-scale use however, is their unaddressed low chemical stability, especially in a high-humidity environment [173,174]. In this case, the *in-situ/operando* investigation became crucial for understanding the mechanisms of their degradation. Adapting the NAP-XPS technique to *in-situ* chemical analysis of perovskite materials under predetermined conditions of exposure to water and oxygen, and defined light illumination, should be beneficial. Recently we performed some preliminary studies on this topic [175] and the results demonstrated a new perspective on this approach, which we would like to develop further.

Besides producing clean energy, it is essential to develop effective mechanisms for its storage and transportation to end-users. A hydrogen economy based on the use of solar energy for hydrogen production by water electrolysis, and its subsequent consumption as a fuel for different types of fuel cells, is now being considered as an option [176–178]. The only issue that prohibits its rapid development is the cost of Pt-based catalysts that are typically used in the Proton-Exchange Membrane (PEM) fuel cells. In the Nanomaterials Group, we are intensively developing and studying potential catalysts for PEM fuel cell applications [35,179,180]. *In-operando* NAP-XPS studies of such catalysts, directly inside the working fuel cell, are highly valued. The potential for such studies was recently demonstrated on pure Pt catalysts (Figure 17) [181]. Thus, recently, we have designed and commenced construction of a special NAP cell, allowing the *operando* investigation of different catalysts for PEM fuel cells using NAP-XPS. This NAP cell will allow us to construct a working fuel cell inside the NAP cell, where one gas (hydrogen, for example) will be supplied to the hidden electrode, and the second gas will be in contact with the open electrode, which NAP-XPS will analyze.

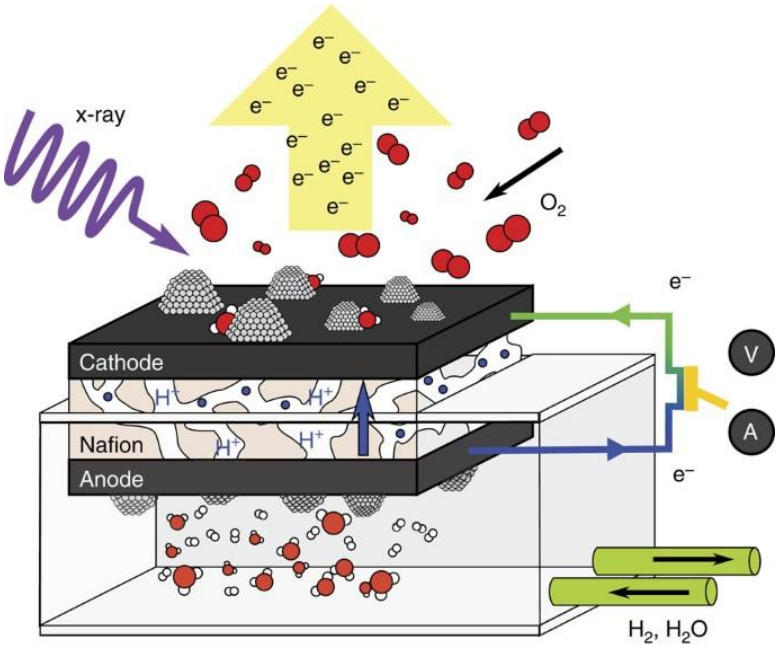

Figure 17. Schematic drawing of a PEM fuel cell set-up for NAPXPS investigations. Reproduced from [181].

7. References

[1] A.C. Luntz, Dynamics of Gas-Surface Interactions, in: K. Wandelt (Ed.), Surf. Interface Sci. Solid-Gas Interfaces II, Wiley-VCH Verlag & Co. KGaA, 2015: pp. 1255–1314. https://doi.org/https://doi.org/10.1007/978-3-642-32955-5.

[2] C. Shen, Interaction of Molecules with Solid Surface, in: D. Mewes, F. Mayinger (Eds.), Rarefied Gas Dyn. Fundam. Simulations Micro Flows, 2005: pp. 131–158. https://doi.org/10.1007/3-540-27230-5_4.

[3] C.T. Rettner, D.J. Auerbach, J.C. Tully, A.W. Kleyn, Chemical dynamics at the gas-surface interface, J. Phys. Chem. 100 (1996) 13021–13033. https://doi.org/10.1021/jp9536007.

[4] A. Adamson, A. Gast, Physical chemistry of surfaces, John Wiley & Sons (Wiley), 1997.

[5] M. Popova, S. Boycheva, H. Lazarova, D. Zgureva, K. Lázár, Á. Szegedi, VOC oxidation and CO2 adsorption on dual adsorption/catalytic system based on fly ash zeolites, Catal. Today. 357 (2020) 518–525. https://doi.org/10.1016/j.cattod.2019.06.070.

[6] P. Pullumbi, F. Brandani, S. Brandani, Gas separation by adsorption: technological drivers and opportunities for improvement, Curr. Opin. Chem. Eng. 24 (2019) 131–142. https://doi.org/10.1016/j.coche.2019.04.008.

[7] S. Brunauer, P.H. Emmett, E. Teller, in Multimolecular, J. Am.Chem.Soc. 60 (1938) 309–319.

[8] J.K. Nørskov, F. Abild-Pedersen, F. Studt, T. Bligaard, Density functional theory in surface chemistry and catalysis, PNAS. 108 (2011) 937–943. https://doi.org/10.1073/pnas.1006652108.

[9] A. Gurlo, Interplay between O2 and SnO2: Oxygen ionosorption and spectroscopic evidence for adsorbed oxygen, ChemPhysChem. 7 (2006) 2041–2052.

[10] K. Oura, V.G. Lifshits, A.A. Saranin, A.V. Zotov, M. Katayama, Surface Science - An Introduction, Springer-Verlag, 2004.

[11] J.R.H. Ross, Heterogeneous Catalysis Fundamentals and Applications, Elsevier, 2004. https://doi.org/https://doi.org/10.1016/C2009-0-19388-1.

[12] F. Cavani, F. Trifiró, Classification of industrial catalysts and catalysis for the petrochemical industry, Catal. Today. 34 (1997) 269–279. https://doi.org/10.1016/s0920-5861(96)00054-5.

[13] F. Devred, P. Dulgheru, N. Kruse, Elementary Steps in Heterogeneous Catalysis, Compr. Inorg. Chem. II (Second Ed. From Elem. to Appl. 7 (2013) 7–38. https://doi.org/10.1016/B978-0-08-097774-4.00703-8.

[14] C. Vogt, B.M. Weckhuysen, The concept of active site in heterogeneous catalysis, Nat. Rev. Chem. 6 (2022) 89–111. https://doi.org/10.1038/s41570-021-00340-y.

[15] A. Zangwill, Physics at Surfaces, Cambridge University Press, 1988. https://doi.org/10.1017/cbo9780511622564.

[16] C.R. Henry, Surface studies of supported model catalysts, Surf. Sci. Rep. 31 (1998) 231–233. https://doi.org/10.1016/S0167-5729(98)00002-8.

[17] B. Qiao, A. Wang, X. Yang, L.F. Allard, Z. Jiang, Y. Cui, J. Liu, J. Li, T. Zhang, Single-atom catalysis of CO oxidation using Pt1/FeOx, Nat. Chem. 3 (2011) 634–641. https://doi.org/10.1038/nchem.1095.

[18] X. Yang, A. Wang, B. Qiao, J.U.N. Li, Single-Atom Catalysts : A New Frontier in Heterogeneous

Catalysis, Acc. Chem. Res. 46 (2013) 1740–1748.

[19] C.H. Bartholomew, Mechanisms of catalyst deactivation, Appl. Catal. A Gen. 212 (2001) 17–60. https://doi.org/10.1016/S0926-860X(00)00843-7.

[20] H. Tang, Y. Su, B. Zhang, A.F. Lee, M.A. Isaacs, K. Wilson, L. Li, Y. Ren, J. Huang, M. Haruta, B. Qiao, X. Liu, C. Jin, D. Su, J. Wang, T. Zhang, Classical strong metal–support interactions between gold nanoparticles and titanium dioxide, Sci. Adv. 3 (2017) 1–9. https://doi.org/10.1126/sciadv.1700231.

[21] X. Liu, M.H. Liu, Y.C. Luo, C.Y. Mou, S.D. Lin, H. Cheng, J.M. Chen, J.F. Lee, T.S. Lin, Strong metal-support interactions between gold nanoparticles and ZnO nanorods in CO oxidation, J. Am. Chem. Soc. 134 (2012) 10251–10258. https://doi.org/10.1021/ja3033235.

[22] P. Trens, R. Durand, B. Coq, C. Coutanceau, S. Rousseau, C. Lamy, Poisoning of Pt/C catalysts by CO and its consequences over the kinetics of hydrogen chemisorption, Appl. Catal. B Environ. 92 (2009) 280–284. https://doi.org/10.1016/j.apcatb.2009.08.004.

[23] D. Avnir, O. Citri, D. Farin, M. Ottolenghi, J. Samuel, A. Seri-Levy, Optimization of Heterogeneous-Catalyst Structure: Simulations and Experiments with Fractal and Non-Fractal Systems, in: Optim. Struct. Heterog. React. Syst., 1989: pp. 65–81. https://doi.org/10.1007/978-3-642-83899-6_3.

[24] R.W. Joyner, Electron Spectroscopy Applied To the Study of Reactivity, Surf. Sci. 63 (1977) 291–314.

[25] J.C. Védrine, Heterogeneous catalysis on metal oxides, Catalysts. 7 (2017) 341. https://doi.org/10.3390/catal7110341.

[26] P. Balla, P.K. Seelam, R. Balaga, R. Rajesh, V. Perupogu, T.X. Liang, Immobilized highly dispersed Ni nanoparticles over porous carbon as an efficient catalyst for selective hydrogenation of furfural and levulinic acid, J. Environ. Chem. Eng. 9 (2021) 106530. https://doi.org/10.1016/j.jece.2021.106530.

[27] L. Liu, A. Corma, Metal Catalysts for Heterogeneous Catalysis: From Single Atoms to Nanoclusters and Nanoparticles, Chem. Rev. 118 (2018) 4981–5079. https://doi.org/10.1021/acs.chemrev.7b00776.

[28] J.M. Escola, J. Aguado, D.P. Serrano, A. García, A. Peral, L. Briones, R. Calvo, E. Fernandez, Catalytic hydroreforming of the polyethylene thermal cracking oil over Ni supported hierarchical zeolites and mesostructured aluminosilicates, Appl. Catal. B Environ. 106 (2011) 405–415. https://doi.org/10.1016/j.apcatb.2011.05.048.

[29] S. Liu, B. Zhang, G. Liu, Metal-based catalysts for the non-oxidative dehydrogenation of light alkanes to light olefins, React. Chem. Eng. 6 (2021) 9–26. https://doi.org/10.1039/d0re00381f.

[30] J. Li, F. Wei, C. Dong, Z. Wang, Z. Xiu, X. Han, Recent progress of inorganic metal-based catalysts in electrocatalytic synthesis of ammonia, Mater. Today Energy. 21 (2021) 100766. https://doi.org/10.1016/j.mtener.2021.100766.

[31] J.A. Rodriguez, P. Liu, D.J. Stacchiola, S.D. Senanayake, M.G. White, J.G. Chen, Hydrogenation of CO2 to Methanol: Importance of Metal-Oxide and Metal-Carbide Interfaces in the Activation of CO2, ACS Catal. 5 (2015) 6696–6706. https://doi.org/10.1021/acscatal.5b01755.

[32] D. Pakhare, J. Spivey, A review of dry (CO2) reforming of methane over noble metal catalysts, Chem. Soc. Rev. 43 (2014) 7813–7837. https://doi.org/10.1039/c3cs60395d.

[33] R. Meyer, C. Lemire, S.K. Shaikhutdinov, H.J. Freund, Surface chemistry of catalysis by gold, Gold Bull. 37 (2004) 72–124. https://doi.org/10.1007/BF03215519.

[34] Y. Lykhach, A. Figueroba, M.F. Camellone, A. Neitzel, T. Skála, F.R. Negreiros, M. Vorokhta, N. Tsud, K.C. Prince, S. Fabris, K.M. Neyman, V. Matolín, J. Libuda, Reactivity of atomically dispersed Pt2+ species towards H2: Model Pt-CeO2 fuel cell catalyst, Phys. Chem. Chem. Phys. 18 (2016) 7672–7679.

[35] R. Fiala, M. Vaclavu, M. Vorokhta, I. Khalakhan, J. Lavkova, V. Potin, I. Matolinova, V. Matolin, Proton exchange membrane fuel cell made of magnetron sputtered Pt-CeOx and Pt-Co thin film catalysts, J. Power Sources. 273 (2015) 105–109. https://doi.org/10.1016/j.jpowsour.2014.08.093.

[36] C. Li, J.B. Baek, Recent Advances in Noble Metal (Pt, Ru, and Ir)-Based Electrocatalysts for Efficient Hydrogen Evolution Reaction, ACS Omega. 5 (2020) 31–40. https://doi.org/10.1021/acsomega.9b03550.

[37] P. Kúš, R. Fiala, M. Václavů, M. Vorokhta, I. Khalakhan, T. Skála, V. Matolín, Low loading magnetron sputtered Pt-IR thin film catalyst for unitized regenerative fuel cell, in: Proc. 6th Eur. Fuel Cell - Piero Lunghi Conf. EFC 2015, 2015.

[38] K. Chakarova, M. Mihaylov, S. Ivanova, M.A. Centeno, K. Hadjiivanov, Well-defined negatively charged gold carbonyls on Au/SiO2, J. Phys. Chem. C. 115 (2011) 21273–21282. https://doi.org/10.1021/jp2070562.

[39] S. Ali, M.J. Al-Marri, A.G. Abdelmoneim, A. Kumar, M.M. Khader, Catalytic evaluation of nickel nanoparticles in methane steam reforming, Int. J. Hydrogen Energy. 41 (2016) 22876–22885. https://doi.org/10.1016/j.ijhydene.2016.08.200.

[40] M. Comotti, W.C. Li, B. Spliethoff, F. Schüth, Support effect in high activity gold catalysts for CO oxidation, J. Am. Chem. Soc. 128 (2006) 917–924. https://doi.org/10.1021/ja0561441.

[41] M. Zhu, P. Tian, R. Kurtz, T. Lunkenbein, J. Xu, R. Schlögl, I.E. Wachs, Y.F. Han, Strong Metal–Support Interactions between Copper and Iron Oxide during the High-Temperature Water-Gas Shift Reaction, Angew. Chemie - Int. Ed. 58 (2019) 9083–9087. https://doi.org/10.1002/anie.201903298.

[42] D. Widmann, R.J. Behm, Active oxygen on a Au/TiO2 catalyst: Formation, stability, and CO oxidation activity, Angew. Chemie - Int. Ed. 50 (2011) 10241–10245. https://doi.org/10.1002/anie.201102062.

[43] N. Ta, J. Liu, S. Chenna, P.A. Crozier, Y. Li, A. Chen, W. Shen, Stabilized gold nanoparticles on ceria nanorods by strong interfacial anchoring, J. Am. Chem. Soc. 134 (2012) 20585–20588. https://doi.org/10.1021/ja310341j.

[44] A.R. Puigdollers, P. Schlexer, S. Tosoni, G. Pacchioni, Increasing oxide reducibility: The role of metal/oxide interfaces in the formation of oxygen vacancies, ACS Catal. 7 (2017) 6493–6513. https://doi.org/10.1021/acscatal.7b01913.

[45] C. Doornkamp, V. Ponec, The universal character of the Mars and Van Krevelen mechanism, J. Mol. Catal. A Chem. 162 (2000) 19–32. https://doi.org/10.1016/S1381-1169(00)00319-8.

[46] T.W. van Deelen, C. Hernández Mejía, K.P. de Jong, Control of metal-support interactions in heterogeneous catalysts to enhance activity and selectivity, Nat. Catal. 2 (2019) 955–970. https://doi.org/10.1038/s41929-019-0364-x.

[47] G.N. Vayssilov, Y. Lykhach, A. Migani, T. Staudt, G.P. Petrova, N. Tsud, T. Skála, A. Bruix, F. Illas, K.C.

Prince, V. Matolín, K.M. Neyman, J. Libuda, Support nanostructure boosts oxygen transfer to catalytically active platinum nanoparticles, Nat. Mater. 10 (2011) 310–315. https://doi.org/10.1038/nmat2976.

[48] R. Goyal, B. Sarkar, A. Bag, N. Siddiqui, D. Dumbre, N. Lucas, S.K. Bhargava, A. Bordoloi, Studies of synergy between metal-support interfaces and selective hydrogenation of HMF to DMF in water, J. Catal. 340 (2016) 248–260. https://doi.org/10.1016/j.jcat.2016.05.012.

[49] J.A. Schwarz, C. Contescu, A. Contescu, Methods for Preparation of Catalytic Materials, Chem. Rev. 95 (1995) 477–510. https://doi.org/10.1021/cr00035a002.

[50] Y.B. Pottathara, Y. Grohens, V. Kokol, N. Kalarikkal, S. Thomas, Synthesis and Processing of Emerging Two-Dimensional Nanomaterials, in: Y. Beeran Pottathara, S. Thomas, N. Kalarikkal, Y. Grohens, V. Kokol (Eds.), Nanomater. Synth., Elsevier, 2019: pp. 1–25. https://doi.org/https://doi.org/10.1016/B978-0-12-815751-0.00001-8.

[51] C. Bock, H. Halvorsen, B. MacDougall, Catalyst Synthesis Techniques, in: J. Zhang (Ed.), PEM Fuel Cell Electrocatal. Catal. Layers Fundam. Appl., Springer London, London, 2008: pp. 447–485. https://doi.org/10.1007/978-1-84800-936-3_9.

[52] P. Munnik, P.E. De Jongh, K.P. De Jong, Recent Developments in the Synthesis of Supported Catalysts, Chem. Rev. 115 (2015) 6687–6718. https://doi.org/10.1021/cr500486u.

[53] V. Meille, Review on methods to deposit catalysts on structured surfaces, Appl. Catal. A Gen. 315 (2006) 1–17. https://doi.org/10.1016/j.apcata.2006.08.031.

[54] W. Huang, W.X. Li, Surface and interface design for heterogeneous catalysis, Phys. Chem. Chem. Phys. 21 (2019) 523–536. https://doi.org/10.1039/c8cp05717f.

[55] A. Ruditskiy, H.C. Peng, Y. Xia, Shape-Controlled Metal Nanocrystals for Heterogeneous Catalysis, Annu. Rev. Chem. Biomol. Eng. 7 (2016) 327–348. https://doi.org/10.1146/annurev-chembioeng-080615-034503.

[56] J. Sauer, H.J. Freund, Models in Catalysis, Catal. Letters. 145 (2015) 109–125. https://doi.org/10.1007/s10562-014-1387-1.

[57] G. Ertl, P. Rau, Chemisorption und katalytische Reaktion von Sauerstoff und Kohlenmonoxid an einer Palladium (110)-Oberfläche, Surf. Sci. 15 (1969) 443–465. https://doi.org/https://doi.org/10.1016/0039-6028(69)90134-4.

[58] J. Polański, Z. Sidorski, Adsorption of copper on tungsten: measurements on single crystal planes, Surf. Sci. 40 (1973) 282–294. https://doi.org/10.1016/0039-6028(73)90068-X.

[59] G. Ertl, S.B. Lee, M. Weiss, Adsorption of nitrogen on potassium promoted Fe(111) and (100) surfaces, Surf. Sci. 114 (1982) 527–545. https://doi.org/https://doi.org/10.1016/0039-6028(82)90703-8.

[60] N.D. Spencer, R.C. Schoonmaker, G.A. Somorjai, Structure sensitivity in the iron single-crystal catalysed synthesis of ammonia, Nature. 294 (1981) 643–644. https://doi.org/10.1038/294643a0.

[61] G. Ertl, Surface Science and Catalysis—Studies on the Mechanism of Ammonia Synthesis: The P. H. Emmett Award Address, Catal. Rev. 21 (1980) 201–223. https://doi.org/10.1080/03602458008067533.

[62] S. Surnev, A. Fortunelli, F.P. Netzer, Structure-property relationship and chemical aspects of oxide-metal hybrid nanostructures, Chem. Rev. 113 (2013) 4314–4372.

https://doi.org/10.1021/cr300307n.

[63] G. Ertl, Reactions at surfaces: From atoms to complexity (nobel lecture), Angew. Chemie - Int. Ed. 47 (2008) 3524–3535. https://doi.org/10.1002/anie.200800480.

[64] D.W. Goodman, Correlations between surface science models and “Real-world” catalysts, J. Phys. Chem. 100 (1996) 13090–13102. https://doi.org/10.1021/jp953755e.

[65] W. Taifan, J.F. Boily, J. Baltrusaitis, Surface chemistry of carbon dioxide revisited, Surf. Sci. Rep. 71 (2016) 595–671. https://doi.org/10.1016/j.surfrep.2016.09.001.

[66] J. Libuda, S. Schauermann, M. Laurin, T. Schalow, H.J. Freund, Model studies in heterogeneous catalysis. From structure to kinetics, Monatshefte Fur Chemie. 136 (2005) 59–75. https://doi.org/10.1007/s00706-004-0249-8.

[67] H.P. Steinrück, J. Libuda, S.A. King, Chemistry at surfaces, Chem. Soc. Rev. 37 (2008) 2153–2154. https://doi.org/10.1039/b814437k.

[68] U. Diebold, S.C. Li, M. Schmid, Oxide surface science, Annu. Rev. Phys. Chem. 61 (2010) 129–148. https://doi.org/10.1146/annurev.physchem.012809.103254.

[69] H. Kuhlenbeck, S. Shaikhutdinov, H.J. Freund, Well-ordered transition metal oxide layers in model catalysis - A series of case studies, Chem. Rev. 113 (2013) 3986–4034. https://doi.org/10.1021/cr300312n.

[70] D.R. Mullins, The surface chemistry of cerium oxide, Surf. Sci. Rep. 70 (2015) 42–85. https://doi.org/10.1016/j.surfrep.2014.12.001.

[71] U. Diebold, <(Surf.Sci.Rep.)[2003]The surface science of titanium dioxide.pdf>, Surf. Sci. Rep. 48 (2002) 53–229. http://linkinghub.elsevier.com/retrieve/pii/S0167572902001000.

[72] J. Dou, Z. Sun, A.A. Opalade, N. Wang, W. Fu, F. Tao, Operando chemistry of catalyst surfaces during catalysis, Chem. Soc. Rev. 46 (2017) 2001–2027. https://doi.org/10.1039/c6cs00931j.

[73] K.F. Kalz, R. Kraehnert, M. Dvoyashkin, R. Dittmeyer, R. Gläser, U. Krewer, K. Reuter, J.D. Grunwaldt, Future Challenges in Heterogeneous Catalysis: Understanding Catalysts under Dynamic Reaction Conditions, ChemCatChem. 9 (2017) 17–29. https://doi.org/10.1002/cctc.201600996.

[74] Y. Zhang, S. Bals, G. Van Tendeloo, Understanding CeO2-Based Nanostructures through Advanced Electron Microscopy in 2D and 3D, Part. Part. Syst. Charact. 36 (2019) 1–32. https://doi.org/10.1002/ppsc.201800287.

[75] L. Lukashuk, K. Foettinger, In situ and operando spectroscopy: A powerful approach towards understanding catalysts, Johnson Matthey Technol. Rev. 62 (2018) 316–331. https://doi.org/10.1595/205651318X15234323420569.

[76] B.M. Weckhuysen, Snapshots of a working catalyst: Possibilities and limitations of in situ spectroscopy in the field of heterogeneous catalysis, Chem. Commun. 2 (2002) 97–110. https://doi.org/10.1039/b107686h.

[77] A. Chakrabarti, M.E. Ford, D. Gregory, R. Hu, C.J. Keturakis, S. Lwin, Y. Tang, Z. Yang, M. Zhu, M.A. Bañares, I.E. Wachs, A decade+ of operando spectroscopy studies, Catal. Today. 283 (2017) 27–53. https://doi.org/10.1016/j.cattod.2016.12.012.

[78] S. Nemšák, E. Strelcov, H. Guo, B.D. Hoskins, T. Duchoň, D.N. Mueller, A. Yulaev, I. Vlassiouk, A. Tselev, C.M. Schneider, A. Kolmakov, In Aqua Electrochemistry Probed by XPEEM: Experimental Setup, Examples, and Challenges, Top. Catal. 61 (2018) 2195–2206.

https://doi.org/10.1007/s11244-018-1065-4.

[79] F. Tao, L. Nguyen, S. Zhang, Design of a new reactor-like high temperature near ambient pressure scanning tunneling microscope for catalysis studies, Rev. Sci. Instrum. 84 (2013) 034101. https://doi.org/10.1063/1.4792673.

[80] K. Föttinger, G. Rupprechter, In situ spectroscopy of complex surface reactions on supported Pd-Zn, Pd-Ga, and Pd(Pt)-Cu nanoparticles, Acc. Chem. Res. 47 (2014) 3071–3079. https://doi.org/10.1021/ar500220v.

[81] Chemical Sensors Based on Semiconductor Electronic Devices, in: Chem. Sensors Biosens., John Wiley & Sons, Ltd, 2012: pp. 217–245. https://doi.org/https://doi.org/10.1002/9781118354162.ch11.

[82] A. Gurlo, Insights into the Mechanism of Gas Sensor Operation, in: M.A. Carpenter, S. Mathur, A. Kolmakov (Eds.), Met. Oxide Nanomater. Chem. Sensors, Springer New York, NY, 2012: pp. 3–34.

[83] S. Pirsa, Chemiresistive gas sensors based on conducting polymers, Mater. Sci. Eng. Concepts, Methodol. Tools, Appl. 1–3 (2017) 543–574. https://doi.org/10.4018/978-1-5225-1798-6.ch022.

[84] T. Han, A. Nag, S. Chandra Mukhopadhyay, Y. Xu, Carbon nanotubes and its gas-sensing applications: A review, Sensors Actuators, A Phys. 291 (2019) 107–143. https://doi.org/10.1016/j.sna.2019.03.053.

[85] H. Nazemi, A. Joseph, J. Park, A. Emadi, Advanced micro-and nano-gas sensor technology: A review, Sensors. 19 (2019) 1285. https://doi.org/10.3390/s19061285.

[86] P. Gründler, Chemical Sensors: An Introduction for Scientists and Engineers, Springer Berlin, Heidelberg, 2007.

[87] T. Seiyama, A. Kato, K. Fujiishi, M. Nagatani, A New Detector for Gaseous Components Using Semiconductive Thin Films, Anal. Chem. 34 (1962) 1502–1503. https://doi.org/10.1021/ac60191a001.

[88] N. Taguchi, A Metal Oxide Gas Sensor, Japan Patent No. 45-38200, 1962.

[89] T.T. Suzuki, T. Ohgaki, Y. Adachi, I. Sakaguchi, M. Nakamura, H. Ohashi, A. Aimi, K. Fujimoto, Ethanol Gas Sensing by a Zn-Terminated ZnO(0001) Bulk Single- Crystalline Substrate, ACS Omega. 5 (2020) 21104–21112. https://doi.org/10.1021/acsomega.0c02750.

[90] T. Tharsika, M. Thanihaichelvan, A.S.M.A. Haseeb, S.A. Akbar, Highly sensitive and selective ethanol sensor based on zno nanorod on SnO2 thin film fabricated by spray pyrolysis, Front. Mater. 6 (2019) 1–9. https://doi.org/10.3389/fmats.2019.00122.

[91] N. Kaur, M. Singh, E. Comini, One-Dimensional Nanostructured Oxide Chemoresistive Sensors, Langmuir. 36 (2020) 6326–6344. https://doi.org/10.1021/acs.langmuir.0c00701.

[92] Y. Masuda, Recent advances in SnO2 nanostructure based gas sensors, Sensors Actuators B Chem. 364 (2022) 131876. https://doi.org/10.1016/j.snb.2022.131876.

[93] N. Yamazoe, New approaches for improving semiconductor gas sensors, Sensors Actuators B Chem. 5 (1991) 7–19. https://doi.org/https://doi.org/10.1016/0925-4005(91)80213-4.

[94] V. Galstyan, A. Moumen, G.W.C. Kumarage, E. Comini, Progress towards chemical gas sensors: Nanowires and 2D semiconductors, Sensors Actuators B Chem. 357 (2022) 131466. https://doi.org/10.1016/j.snb.2022.131466.

[95] A. Sharma, C.S. Rout, Advances in understanding the gas sensing mechanisms byin situandoperandospectroscopy, J. Mater. Chem. A. 9 (2021) 18175–18207. https://doi.org/10.1039/d1ta05054k.

[96] Y. Shimizu, SnO2 Gas Sensor, in: G. Kreysa, K. Ota, R.F. Savinell (Eds.), Encycl. Appl. Electrochem., Springer New York, New York, NY, 2014: pp. 1974–1982. https://doi.org/10.1007/978-1-4419-6996-5_475.

[97] H.J. Kim, J.H. Lee, Highly sensitive and selective gas sensors using p-type oxide semiconductors: Overview, Sensors Actuators, B Chem. 192 (2014) 607–627. https://doi.org/10.1016/j.snb.2013.11.005.

[98] A.A. Abokifa, K. Haddad, J. Fortner, C.S. Lo, P. Biswas, Sensing mechanism of ethanol and acetone at room temperature by SnO2 nano-columns synthesized by aerosol routes: theoretical calculations compared to experimental results, J. Mater. Chem. A. 6 (2018) 2053–2066.

[99] Y. Chen, C.L. Zhu, G. Xiao, Reduced-temperature ethanol sensing characteristics of flower-like ZnO nanorods synthesized by a sonochemical method, Nanotechnology. 17 (2006) 4537–4541. https://doi.org/10.1088/0957-4484/17/18/002.

[100] S. Kucharski, P. Ferrer, F. Venturini, G. Held, A.S. Walton, C. Byrne, J.A. Covington, S.K. Ayyala, A.M. Beale, C. Blackman, Direct in situ spectroscopic evidence of the crucial role played by surface oxygen vacancies in the O2-sensing mechanism of SnO2, Chem. Sci. 13 (2022) 6089–6097. https://doi.org/10.1039/d2sc01738e.

[101] L.-Y. Guo, S. Liang, Z. Yang, L. Jin, Y. Tan, Z. Huang, Gas-Sensing Properties of Dissolved Gases in Insulating Material Adsorbed on SnO2–GeSe Monolayer, Chemosensors. 10 (2022) 212. https://doi.org/10.3390/chemosensors10060212.

[102] A. Gurlo, R. Riedel, In situ and operando spectroscopy for assessing mechanisms of gas sensing, Angew. Chemie - Int. Ed. 46 (2007) 3826–3848.

[103] D. Wöhrle, L. Kreienhoop, D. Schlettwein, Phthalocyanines and related Macrocycles in Organic Phototovoltaic Junctions. In Phthalocyanines, Properties, and Applications, VCH Publishers Inc., New York, 1996.

[104] R.R. Cranston, B.H. Lessard, Metal phthalocyanines: thin-film formation, microstructure, and physical properties, RSC Adv. 11 (2021) 21716–21737. https://doi.org/10.1039/d1ra03853b.

[105] M.S. Liao, S. Scheiner, Electronic structure and bonding in metal phthalocyanines, metal=Fe, Co, Ni, Cu, Zn, Mg, J. Chem. Phys. 114 (2001) 9780–9791. https://doi.org/10.1063/1.1367374.

[106] D.D. Eley, D.J. Hazeldine, T.F. Palmer, MASS-SPECTRA, IONIZATION-POTENTIALS AND RELATED PROPERTIES OF METAL-FREE AND TRANSITION-METAL PHTHALOCYANINES, J. Chem. Soc. Trans. II. 69 (1973) 1808–1814. https://doi.org/10.1039/F29736901808.

[107] E. Tegeler, M. Iwan, E.-E. Koch, Electronic structure of the valence bands of H2-, Mg- and Pt-phthalocyanine derived from soft X-ray emission and photoelectron emission spectra, J. Electron Spectros. Relat. Phenomena. 22 (1981) 297–307. https://doi.org/https://doi.org/10.1016/0368-2048(81)85020-7.

[108] P. Gregory, Industrial applications of phthalocyanines, J. Porphyr. Phthalocyanines. 4 (2000) 432–437. https://doi.org/10.1002/(SICI)1099-1409(200006/07)4:4<432::AID-JPP254>3.3.CO;2-E.

[109] E. Vesselli, Tetrapyrroles at near-ambient pressure: Porphyrins and phthalocyanines beyond the pressure gap, J. Phys. Mater. 3 (2020) 022002. https://doi.org/10.1088/2515-7639/ab7ab2.

[110] A. Rydosz, E. Maciak, K. Wincza, S. Gruszczynski, Microwave-based sensors with phthalocyanine films for acetone, ethanol and methanol detection, Sensors Actuators, B Chem. 237 (2016) 876–886. https://doi.org/10.1016/j.snb.2016.06.168.

[111] J. Rossignol, G. Barochi, B. De Fonseca, J. Brunet, M. Bouvet, A. Pauly, L. Markey, Microwave-based gas sensor with phthalocyanine film at room temperature, Sensors Actuators, B Chem. 189 (2013) 213–216. https://doi.org/10.1016/j.snb.2013.03.092.

[112] J. Brunet, V.P. Garcia, A. Pauly, C. Varenne, B. Lauron, An optimised gas sensor microsystem for accurate and real-time measurement of nitrogen dioxide at ppb level, Sensors Actuators, B Chem. 134 (2008) 632–639. https://doi.org/10.1016/j.snb.2008.06.010.

[113] A. Wilson, J.D. Wright, Understanding and optimising no2-sensing using semiconducting phthalocyanine films, Mol. Cryst. Liq. Cryst. Sci. Technol. Sect. A. Mol. Cryst. Liq. Cryst. 211 (1992) 321–326. https://doi.org/10.1080/10587259208025831.

[114] Q. Zhou, R.D. Gould, A study of the response rate to nitrogen dioxide exposure in metal phthalocyanine thin film sensors, Thin Solid Films. 317 (1998) 436–439. https://doi.org/10.1016/S0040-6090(97)00580-4.

[115] A.R. Jalil, H. Chang, V.K. Bandari, P. Robaschik, J. Zhang, P.F. Siles, G. Li, D. Bürger, D. Grimm, X. Liu, G. Salvan, D.R.T. Zahn, F. Zhu, H. Wang, D. Yan, O.G. Schmidt, Fully Integrated Organic Nanocrystal Diode as High Performance Room Temperature NO2 Sensor, Adv. Mater. 28 (2016) 2971–2977. https://doi.org/10.1002/adma.201506293.

[116] M.I. Newton, T.K.H. Starke, M.R. Willis, G. McHale, NO2 detection at room temperature with copper phthalocyanine thin film devices, Sensors Actuators, B Chem. 67 (2000) 307–311. https://doi.org/10.1016/S0925-4005(00)00542-6.

[117] A. Wilson, J.D. Wright, A. V. Chadwick, A microprocessor-controlled nitrogen dioxide sensing system, Sensors Actuators B. Chem. 4 (1991) 499–504. https://doi.org/10.1016/0925-4005(91)80158-G.

[118] D. Tomecek, M. Hruska, P. Fitl, J. Vlcek, E. Maresova, S. Havlova, L. Patrone, M. Vrnata, Phthalocyanine Photoregeneration for Low Power Consumption Chemiresistors, ACS Sensors. 3 (2018) 2558–2565. https://doi.org/10.1021/acssensors.8b00922.

[119] J.D. Wright, Gas adsorption on phthalocyanines and its effects on electrical properties, Prog. Surf. Sci. 31 (1989) 1–60. https://doi.org/10.1016/0079-6816(89)90012-9.

[120] J. Park, J.E. Royer, C.N. Colesniuc, F.I. Bohrer, A. Sharoni, S. Jin, I.K. Schuller, W.C. Trogler, A.C. Kummel, Ambient induced degradation and chemically activated recovery in copper phthalocyanine thin film transistors, J. Appl. Phys. 106 (2009) 034505. https://doi.org/10.1063/1.3159885.

[121] J.H. Park, J.E. Royer, E. Chagarov, T. Kaufman-Osborn, M. Edmonds, T. Kent, S. Lee, W.C. Trogler, A.C. Kummel, Atomic imaging of the irreversible sensing mechanism of NO2 adsorption on copper phthalocyanine, J. Am. Chem. Soc. 135 (2013) 14600–14609. https://doi.org/10.1021/ja403752r.

[122] L.S. Chia, Y.H. Du, S. Palale, P.S. Lee, Interaction of Copper Phthalocyanine with Nitrogen Dioxide and Ammonia Investigation Using X-ray Absorption Spectroscopy and Chemiresistive Gas Measurements, ACS Omega. 4 (2019) 10388–10395. https://doi.org/10.1021/acsomega.8b02108.

[123] N. Padma, A. Joshi, A. Singh, S.K. Deshpande, D.K. Aswal, S.K. Gupta, J. V. Yakhmi, NO2 sensors with room temperature operation and long term stability using copper phthalocyanine thin films,

Sensors Actuators, B Chem. 143 (2009) 246–252. https://doi.org/10.1016/j.snb.2009.07.044.

[124] D. Briggs, X-ray photoelectron spectroscopy (XPS), Handb. Adhes. Second Ed. (2005) 621–622. https://doi.org/10.1002/0470014229.ch22.

[125] H. Yamamoto, Y. Yamada, M. Sasase, F. Esaka, Non-destructive depth profile analysis for surface and buried interface of Ge thin film on Si substrate by high-energy synchrotron radiation x-ray photoelectron spectroscopy, J. Phys. Conf. Ser. 100 (2008). https://doi.org/10.1088/1742-6596/100/1/012044.

[126] D.H. Bilderback, P. Elleaume, E. Weckert, Review of third and next generation synchrotron light sources, J. Phys. B At. Mol. Opt. Phys. 38 (2005) 773–797. https://doi.org/10.1088/0953-4075/38/9/022.

[127] I. Lindgren, Chemical shifts in X-ray and photo-electron spectroscopy: A historical review, J. Electron Spectros. Relat. Phenomena. 137–140 (2004) 59–71. https://doi.org/10.1016/j.elspec.2004.02.086.

[128] K. Siegbahn, Electron Spectroscopy for Chemical Analysis, in: S.J. Smith, G.K. Walters (Eds.), At. Phys. 3, Springer US, Boston, MA, 1973: pp. 493–522.

[129] I. Matolínová, V. Johánek, J. Mysliveček, K.C. Prince, T. Skála, M. Škoda, N. Tsud, M. Vorokhta, V. Matolín, CO and methanol adsorption on (2 × 1)Pt(110) and ion-eroded Pt(111) model catalysts, Surf. Interface Anal. 43 (2011) 1325–1331. https://doi.org/10.1002/sia.3717.

[130] A. Neitzel, Y. Lykhach, T. Skála, N. Tsud, V. Johánek, M. Vorokhta, K.C. Prince, V. Matolín, J. Libuda, Hydrogen activation on Pt-Sn nanoalloys supported on mixed Sn-Ce oxide films., Phys. Chem. Chem. Phys. 16 (2014) 13209–19. https://doi.org/https://doi.org/10.1039/C4CP01632G.

[131] A.R. Head, H. Bluhm, Ambient pressure x-ray photoelectron spectroscopy, Elsevier, 2018. https://doi.org/10.1016/B978-0-12-409547-2.10924-2.

[132] N. Martensson, A. Föhlisch, S. Svensson, Uppsala and Berkeley: Two essential laboratories in the development of modern photoelectron spectroscopy, J. Vac. Sci. Technol. A. 40 (2022) 043207. https://doi.org/10.1116/6.0001879.

[133] R.W. Joyner, M.W. Roberts, K. Yates, A “high-pressure” electron spectrometer for surface studies, Surf. Sci. 87 (1979) 501–509. https://doi.org/https://doi.org/10.1016/0039-6028(79)90544-2.

[134] O. Karsl\io\uglu, H. Bluhm, Ambient-Pressure X-ray Photoelectron Spectroscopy (APXPS), in: J. Frenken, I. Groot (Eds.), Operando Res. Heterog. Catal., Springer International Publishing, Cham, 2017: pp. 31–57. https://doi.org/10.1007/978-3-319-44439-0_2.

[135] D.E. Starr, H. Bluhm, Z. Liu, A. Knop-gericke, M. Hävecker, Application of Ambient-Pressure X-ray Photoelectron Spectroscopy for the In-situ Investigation of Heterogeneous Catalytic Reactions, in: J.A. Rodriguesz, J.C. Hanson, P.J. Chupas (Eds.), In-Situ Charact. Heterog. Catal., Wiley: Hoboken, 2013: pp. 315–343.

[136] D.F. Ogletree, H. Bluhm, G. Lebedev, C.S. Fadley, Z. Hussain, M. Salmeron, A differentially pumped electrostatic lens system for photoemission studies in the millibar range, Rev. Sci. Instrum. 73 (2002) 3872. https://doi.org/10.1063/1.1512336.

[137] G. Kim, Y. Yu, H. Lim, B. Jeong, J. Lee, J. Baik, B.S. Mun, K. Kim, AP-XPS beamline, a platform for operando science at Pohang Accelerator Laboratory, J. Synchrotron Radiat. 27 (2020) 507–514. https://doi.org/10.1107/S160057751901676X.

[138] J. Schnadt, J. Knudsen, J.N. Andersen, H. Siegbahn, A. Pietzsch, F. Hennies, N. Johansson, N. Mårtensson, G. Öhrwall, S. Bahr, S. Mähl, O. Schaff, The new ambient-pressure X-ray photoelectron spectroscopy instrument at MAX-lab, J. Synchrotron Radiat. 19 (2012) 701–704.

[139] C. Arble, M. Jia, J.T. Newberg, Lab-based ambient pressure X-ray photoelectron spectroscopy from past to present, Surf. Sci. Rep. 73 (2018) 37–57. https://doi.org/https://doi.org/10.1016/j.surfrep.2018.02.002.

[140] H. Bluhm, Photoelectron spectroscopy of surfaces under humid conditions, J. Electron Spectros. Relat. Phenomena. 177 (2010) 71–84. https://doi.org/https://doi.org/10.1016/j.elspec.2009.08.006.

[141] V. Matolín, J. Libra, I. Matolínová, V. Nehasil, L. Sedláček, F. Šutara, Growth of ultra-thin cerium oxide layers on Cu(1 1 1), Appl. Surf. Sci. 254 (2007) 153–155. https://doi.org/10.1016/j.apsusc.2007.07.010.

[142] T. Duchoň, F. Dvořák, M. Aulická, V. Stetsovych, M. Vorokhta, D. Mazur, K. Veltruská, T. Skála, J. Mysliveček, I. Matolínová, V. Matolín, Ordered phases of reduced ceria as epitaxial films on Cu(111), J. Phys. Chem. C. 118 (2014) 357–365. https://doi.org/10.1021/jp409220p.

[143] F. Dvořák, M.F. Camellone, A. Tovt, N. Tran, F.R. Negreiros, M. Vorokhta, T. Skála, I. Matolínová, J. Mysliveček, V. Matolín, S. Fabris, Creating single-atom Pt-ceria catalysts by surface step decoration, Nat. Commun. 7 (2016) 1–8.

[144] F. Dvorak, L. Szabova, V. Johánek, M. Farnesi Camellone, V. Stetsovych, M. Vorokhta, A. Tovt, T. Skála, I. Matolínová, Y. Tateyama, J. Myslivecek, S. Fabris, V. Matolín, Bulk Hydroxylation and Effective Water Splitting by Highly Reduced Cerium Oxide: The Role of O Vacancy Coordination, ACS Catal. 8 (n.d.) 4354–4363. https://doi.org/10.1021/acscatal.7b04409.

[145] A. Trovarelli, Catalysis by Ceria and Related Materials, IMPERIAL COLLEGE PRESS, 2012. https://doi.org/doi:10.1142/p870.

[146] S. Gatla, D. Aubert, G. Agostini, O. Mathon, S. Pascarelli, T. Lunkenbein, M.G. Willinger, H. Kaper, Room-Temperature CO Oxidation Catalyst: Low-Temperature Metal-Support Interaction between Platinum Nanoparticles and Nanosized Ceria, ACS Catal. 6 (2016) 6151–6155. https://doi.org/10.1021/acscatal.6b00677.

[147] C. Sun, H. Li, L. Chen, Nanostructured ceria-based materials: synthesis, properties, and applications, Energy Environ. Sci. 5 (2012) 8475–8505. https://doi.org/10.1039/C2EE22310D.

[148] L. Nie, D. Mei, H. Xiong, B. Peng, Z. Ren, X.I. Pereira Hernandez, A. Delariva, M. Wang, M.H. Engelhard, L. Kovarik, A.K. Datye, † Yong Wang, Activation of surface lattice oxygen in single-atom Pt/CeO2 for low-temperature CO oxidation, Science. 358 (2017) 1419–1423. https://doi.org/10.1126/science.aao2109.

[149] D. Li, L. Zeng, X. Li, X. Wang, H. Ma, S. Assabumrungrat, J. Gong, Ceria-promoted Ni/SBA-15 catalysts for ethanol steam reforming with enhanced activity and resistance to deactivation, Appl. Catal. B Environ. 176–177 (2015) 532–541. https://doi.org/10.1016/j.apcatb.2015.04.020.

[150] Y. Lyu, J.N. Jocz, R. Xu, O.C. Williams, C. Sievers, Selective Oxidation of Methane to Methanol over Ceria-Zirconia Supported Mono and Bimetallic Transition Metal Oxide Catalysts, ChemCatChem. 13 (2021) 2832–2842. https://doi.org/10.1002/cctc.202100268.

[151] A. Trovarelli, J. Llorca, Ceria Catalysts at Nanoscale: How Do Crystal Shapes Shape Catalysis?, ACS Catal. 7 (2017) 4716–4735. https://doi.org/10.1021/acscatal.7b01246.

[152] Y. Lin, Z. Wu, J. Wen, K. Ding, X. Yang, K.R. Poeppelmeier, L.D. Marks, Adhesion and Atomic Structures of Gold on Ceria Nanostructures: The Role of Surface Structure and Oxidation State of Ceria Supports, Nano Lett. 15 (2015) 5375–5381. https://doi.org/10.1021/acs.nanolett.5b02694.

[153] A. Basile, Methane in the Environment: Occurence, Uses and Pollution, Nova Science Publication Inc, 2013.

[154] M. Haruta, S. Tsubota, T. Kobayashi, H. Kageyama, M.J. Genet, B. Delmon, Low-temperature oxidation of CO over gold supported on TiO2, α-Fe2O3, and Co3O4, J. Catal. 144 (1993) 175–192. https://doi.org/10.1006/jcat.1993.1322.

[155] Q. Fu, A. Weber, M. Flytzani-Stephanopoulos, Nanostructured Au-CeO2 catalysts for low-temperature water-gas shift, Catal. Letters. 77 (2001) 87–95. https://doi.org/10.1023/A:1012666128812.

[156] X.S. Huang, H. Sun, L.C. Wang, Y.M. Liu, K.N. Fan, Y. Cao, Morphology effects of nanoscale ceria on the activity of Au/CeO2 catalysts for low-temperature CO oxidation, Appl. Catal. B Environ. 90 (2009) 224–232. https://doi.org/10.1016/j.apcatb.2009.03.015.

[157] H.Y. Kim, G. Henkelman, CO oxidation at the interface of au nanoclusters and the stepped-CeO 2(111) surface by the Mars-van Krevelen mechanism, J. Phys. Chem. Lett. 4 (2013) 216–221. https://doi.org/10.1021/jz301778b.

[158] Y.G. Wang, D. Mei, V.A. Glezakou, J. Li, R. Rousseau, Dynamic formation of single-atom catalytic active sites on ceria-supported gold nanoparticles, Nat. Commun. 6 (2015) 1–8. https://doi.org/10.1038/ncomms7511.

[159] L.W. Guo, P.P. Du, X.P. Fu, C. Ma, J. Zeng, R. Si, Y.Y. Huang, C.J. Jia, Y.W. Zhang, C.H. Yan, Contributions of distinct gold species to catalytic reactivity for carbon monoxide oxidation, Nat. Commun. 7 (2016) 13481. https://doi.org/10.1038/ncomms13481.

[160] J. Guzman, S. Carrettin, A. Corma, Spectroscopic evidence for the supply of reactive oxygen during CO oxidation catalyzed by gold supported on nanocrystalline CeO2, J. Am. Chem. Soc. 127 (2005) 3286–3287. https://doi.org/10.1021/ja043752s.

[161] M. Ziemba, C. Schilling, M.V. Ganduglia-Pirovano, C. Hess, Toward an Atomic-Level Understanding of Ceria-Based Catalysts: When Experiment and Theory Go Hand in Hand, Acc. Chem. Res. 54 (2021) 2884–2893. https://doi.org/10.1021/acs.accounts.1c00226.

[162] F.F. Muñoz, L.M. Acuña, C.A. Albornoz, A.G. Leyva, R.T. Baker, R.O. Fuentes, Redox properties of nanostructured lanthanide-doped ceria spheres prepared by microwave assisted hydrothermal homogeneous co-precipitation, Nanoscale. 7 (2015) 271–281. https://doi.org/10.1039/c4nr05630b.

[163] O. Bezkrovnyi, P. Kraszkiewicz, I. Krivtsov, J. Quesada, S. Ordóñez, L. Kepinski, Thermally induced sintering and redispersion of Au nanoparticles supported on Ce1-xEuxO2 nanocubes and their influence on catalytic CO oxidation, Catal. Commun. 131 (2019) 105798. https://doi.org/10.1016/j.catcom.2019.105798.

[164] S. Fernández-García, S.E. Collins, M. Tinoco, A.B. Hungría, J.J. Calvino, M.A. Cauqui, X. Chen, Influence of {111} nanofaceting on the dynamics of CO adsorption and oxidation over Au supported on CeO2 nanocubes: An operando DRIFT insight, Catal. Today. 336 (2019) 90–98. https://doi.org/10.1016/j.cattod.2019.01.078.

[165] A. Tovt, L. Bagolini, F. Dvořák, N.D. Tran, M. Vorokhta, K. Beranová, V. Johánek, M. Farnesi

Camellone, T. Skála, I. Matolínová, J. Mysliveček, S. Fabris, V. Matolín, Ultimate dispersion of metallic and ionic platinum on ceria, J. Mater. Chem. A. 7 (2019) 13019–13028. https://doi.org/10.1039/c9ta00823c.

[166] S. Aouad, E. Saab, E. Abi Aad, A. Aboukaïs, Reactivity of Ru-based catalysts in the oxidation of propene and carbon black, Catal. Today. 119 (2007) 273–277. https://doi.org/10.1016/j.cattod.2006.08.030.

[167] A. Aitbekova, L. Wu, C.J. Wrasman, A. Boubnov, A.S. Hoffman, E.D. Goodman, S.R. Bare, M. Cargnello, Low-Temperature Restructuring of CeO2-Supported Ru Nanoparticles Determines Selectivity in CO2 Catalytic Reduction, J. Am. Chem. Soc. 140 (2018) 13736–13745. https://doi.org/10.1021/jacs.8b07615.

[168] D. Kohl, Surface processes in the detection of reducing gases with SnO2-based devices, Sensors Actuators B. 18 (1989) 71–113.

[169] A. Rydosz, The Use of Copper Oxide Thin Films in Gas-Sensing Applications, Coatings. 8 (2018) 425. https://doi.org/10.3390/coatings8120425.

[170] H. Zhang, Q. Zhu, Y. Zhang, Y. Wang, L. Zhao, B. Yu, One-pot synthesis and hierarchical assembly of hollow Cu2O microspheres with nanocrystals-composed porous multishell and their gas-sensing properties, Adv. Funct. Mater. 17 (2007) 2766–2771. https://doi.org/10.1002/adfm.200601146.

[171] S. Chu, A. Majumdar, Opportunities and challenges for a sustainable energy future, Nature. 488 (2012) 294–303. https://doi.org/10.1038/nature11475.

[172] T. Du, T.J. Macdonald, R.X. Yang, M. Li, Z. Jiang, L. Mohan, W. Xu, Z. Su, X. Gao, R. Whiteley, C.T. Lin, G. Min, S.A. Haque, J.R. Durrant, K.A. Persson, M.A. McLachlan, J. Briscoe, Additive-Free, Low-Temperature Crystallization of Stable α-FAPbI3 Perovskite, Adv. Mater. 34 (2022) 1–10. https://doi.org/10.1002/adma.202107850.

[173] M. V. Khenkin, E.A. Katz, A. Abate, G. Bardizza, J.J. Berry, C. Brabec, F. Brunetti, V. Bulović, Q. Burlingame, A. Di Carlo, R. Cheacharoen, Y.B. Cheng, A. Colsmann, S. Cros, K. Domanski, M. Dusza, C.J. Fell, S.R. Forrest, Y. Galagan, D. Di Girolamo, M. Grätzel, A. Hagfeldt, E. von Hauff, H. Hoppe, J. Kettle, H. Köbler, M.S. Leite, S. (Frank) Liu, Y.L. Loo, J.M. Luther, C.Q. Ma, M. Madsen, M. Manceau, M. Matheron, M. McGehee, R. Meitzner, M.K. Nazeeruddin, A.F. Nogueira, Ç. Odabaşı, A. Osherov, N.G. Park, M.O. Reese, F. De Rossi, M. Saliba, U.S. Schubert, H.J. Snaith, S.D. Stranks, W. Tress, P.A. Troshin, V. Turkovic, S. Veenstra, I. Visoly-Fisher, A. Walsh, T. Watson, H. Xie, R. Yıldırım, S.M. Zakeeruddin, K. Zhu, M. Lira-Cantu, Consensus statement for stability assessment and reporting for perovskite photovoltaics based on ISOS procedures, Nat. Energy. 5 (2020) 35–49. https://doi.org/10.1038/s41560-019-0529-5.

[174] A. Mahapatra, D. Prochowicz, M.M. Tavakoli, S. Trivedi, P. Kumar, P. Yadav, A review of aspects of additive engineering in perovskite solar cells, J. Mater. Chem. A. 8 (2020) 27–54. https://doi.org/10.1039/c9ta07657c.

[175] M. Kot, M. Vorokhta, Z. Wang, H.J. Snaith, D. Schmeißer, J.I. Flege, Thermal stability of CH3NH3PbIxCl3-x versus [HC(NH2)2]0.83Cs0.17PbI2.7Br0.3 perovskite films by X-ray photoelectron spectroscopy, Appl. Surf. Sci. 513 (2020) 145596. https://doi.org/10.1016/j.apsusc.2020.145596.

[176] I. Staffell, D. Scamman, A. Velazquez Abad, P. Balcombe, P.E. Dodds, P. Ekins, N. Shah, K.R. Ward, The role of hydrogen and fuel cells in the global energy system, Energy Environ. Sci. 12 (2019) 463–491. https://doi.org/10.1039/c8ee01157e.

[177] M. Carmo, D.L. Fritz, J. Mergel, D. Stolten, A comprehensive review on PEM water electrolysis, Int. J. Hydrogen Energy. 38 (2013) 4901–4934. https://doi.org/10.1016/j.ijhydene.2013.01.151.

[178] X. Li, L. Zhao, J. Yu, X. Liu, X. Zhang, H. Liu, W. Zhou, Water Splitting: From Electrode to Green Energy System, Nano-Micro Lett. 12 (2020) 1–29. https://doi.org/10.1007/s40820-020-00469-3.

[179] R. Fiala, M. Vaclavu, A. Rednyk, I. Khalakhan, M. Vorokhta, J. Lavkova, V. Potin, I. Matolinova, V. Matolin, Pt-CeOx thin film catalysts for PEMFC, Catal. Today. 240 (2015) 236–241. https://doi.org/10.1016/j.cattod.2014.03.069.

[180] R. Fiala, A. Figueroba, A. Bruix, M. Vaclavu, A. Rednyk, I. Khalakhan, M. Vorokhta, J. Lavkova, F. Illas, V. Potin, I. Matolinova, K.M. Neyman, V. Matolin, High efficiency of Pt2+- CeO2 novel thin film catalyst as anode for proton exchange membrane fuel cells, Appl. Catal. B Environ. 197 (2016) 262–270. https://doi.org/10.1016/j.apcatb.2016.02.036.

[181] H.S. Casalongue, S. Kaya, V. Viswanathan, D.J. Miller, D. Friebel, H.A. Hansen, J.K. Nørskov, A. Nilsson, H. Ogasawara, Direct observation of the oxygenated species during oxygen reduction on a platinum fuel cell cathode, Nat. Commun. 4 (2013) 2817. https://doi.org/10.1038/ncomms3817.

8. List of Abbreviations

AC	Alternating Current
ALD	Atomic Layer Deposition
ALS	Advanced Light Source
BNL	Brookhaven National Laboratory
CVD	Chemical Vapor Deposition
DRIFTS	Diffuse Reflectance Infrared Fourier Transform Spectroscopy
DRM	Dry Reforming of Methane
DFT	Density Functional Theory
EC	Electrochemical
ESCA	Electron Spectroscopy for Chemical Analysis
E-SEM	Environmental Scanning Electron Microscopy
E-TEM	Environmental Transmission Electron Microscopy
HP-STM	High-Pressure Scanning Tunneling Microscopy
IMFP	Inelastic Mean Free Path
IR	Infrared Spectroscopy
LEED	Low-Energy Electron Diffraction
LED	Light-Emitting Diode
MOX	Metal-Oxide
MSI	Metal-Support Interaction
NAP-XPS	Near-Ambient Pressure X-ray Photoelectron Spectroscopy
NPs	Nanoparticles
NRs	Nanorods
NWs	Nanowires
PVD	Physical Vapor Deposition
SRPES	Synchrotron Radiation Photoelectron Spectroscopy
STM	Scanning Tunneling Microscopy
TEM	Scanning Transmission Microscopy
UHV	Ultra-High Vacuum
VOCs	Volatile Organic Compounds
ZnPc	Zn-Phthalocyanine

9. List of selected publications

A1. Liu, Z; Lustemberg, P; Gutiérrez, RA; Carey, JJ; Palomino, RM; Vorokhta, M; Grinter, DC; Ramírez, PJ; Matolín, V; Nolan, M; Ganduglia-Pirovano, V; Senanayake, SD; Rodriguez, JA. In Situ Investigation of Methane Dry Reforming on Metal/Ceria(111) Surfaces: Metal–Support Interactions and C−H Bond Activation at Low Temperature, *Angew. Chem.-Int. Edit.*, 56, 42, 13041–13046, 2017. DOI: 10.1002/anie.201707538.

A2. Lustemberg, PG; Palomino, RM; Gutiérrez, RA; Grinter, DC; Vorokhta, M; Liu, Z; Ramírez, PJ; Matolín, V; Ganduglia-Pirovano, MV; Senanayake, SD; Rodriguez, JA, Direct Conversion of Methane to Methanol on Ni-Ceria Surfaces: Metal–Support Interactions and Water-Enabled Catalytic Conversion by Site Blocking, *J. Am. Chem. Soc.*, 140, 24, 7681–7687, 2018. DOI: 10.1021/jacs.8b03809.

A3. Vorokhta, M; Khalakhan, I; Vondráček, M; Tomeček, D; Vorokhta, M; Marešová, E; Nováková, J; Vlček, J; Fitl, P; Novotný, M; Hozák, P; Lančok, J; Vrňata, M; Matolínová, I; Matolín, V. Investigation of Gas Sensing Mechanism of SnO_2 Based Chemiresistor using Near Ambient Pressure XPS, *Surf. Sci.*, 677, 284–290, 2018. DOI: 10.1016/j.susc.2018.08.003.

A4. Hozák, P; Vorokhta, M; Khalakhan, I; Jarkovská, K; Cibulková, J; Fitl, P; Vlček, J; Fara, J; Tomeček, D; Novotný, M; Vorokhta, M; Lančok, J; Matolínová, I; Vrňata, M. New Insight into the Gas-Sensing Properties of CuO_x Nanowires by Near-Ambient Pressure XPS. *J. Phys. Chem. C*, 123, 49, 29739–29749, 2019. DOI: 10.1021/acs.jpcc.9b09124.

A5. Bezrkovnyi, OS; Vorokhta, M; Małecka, M; Mista, W; Kepinski, L. NAP-XPS Study of $Eu^{3+} \rightarrow Eu^{2+}$ and $Ce^{4+} \rightarrow Ce^{3+}$ Reduction in $Au/Ce_{0.8}Eu_{0.2}O_2$ Catalyst. *Catalysis Communications*, 135, 105875, 2020. DOI: 10.1016/j.catcom.2019.105875.

A6. O. S. Bezkrovnyi, D. Blaumeiser, M. Vorokhta, P. Kraszkiewicz, M. Pawlyta, T. Bauer, J. Libuda, L. Kepinski, NAP-XPS and In Situ DRIFTS of the Interaction of CO with Au Nanoparticles Supported by $Ce_{1-x}Eu_xO_2$ Nanocubes, *J. Phys. Chem. C*, 124, 10, 5647-5656, 2020. DOI: 10.1021/acs.jpcc.9b10142.

A7. Piliai, L; Tomeček, D; Hruška, M; Khalakhan, I; Nováková, J; Fitl, P; Yatskiv, R; Grym, J; Vorokhta, M; Matolínová, I; Vrňata, M. New Insights towards High-Temperature Ethanol-Sensing Mechanism of ZnO-Based Chemiresistors. *Sensors*, 20, 19, 5602, 2020. DOI: doi.org/10.3390/s20195602.

A8. Tomeček, D.; Piliai, L.; Hruška, M.; Fitl, P.; Gadenne, V.; Vorokhta, M.; Matolínová, I.; Vrňata, M. Study of Photoregeneration of Zinc Phthalocyanine Chemiresistor after Exposure to Nitrogen Dioxide. *Chemosensors*, 9, 9, 237, 2021. DOI: doi.org/10.3390/chemosensors9090237.

A9. Meunier, FC; Cardenas, L; Kaper, H; Šmíd, B; Vorokhta, M; Grosjean, R; Aubert, D; Dembélé, K; Lunkenbein, T. Synergy between Metallic and Oxidized Pt Sites Unravelled during Room Temperature CO Oxidation on Pt/Ceria. *Angew. Chem. Int. Ed.*, 60, 7, 3799–3805, 2021. DOI: doi.org/10.1002/anie.202013223.

A10. Bezkrovnyi, OS; Vorokhta, M; Pawlyta, M; Ptak, M; Piliai, L; Xie, X; Dinhová, T.H.; Matolínová, I; Kepinski, L. In-situ study of Ru/CeO_2 catalyst under propane oxidation. *J. Mater. Chem. A,* 10, 31, 16675-16684, 2022. DOI: 10.1039/D2TA02330J.

A11. Bezkrovnyi, O; Bruix, A; Blaumeiser, D; Piliai, L; Schötz, S; Bauer, T; Khalakhan, I; Skála, T; Matvija, P; Kraszkiewicz, P; Pawlyta, M; Vorokhta, M; Matolínová, I; Libuda, J; Neyman, KM; Kępiński, L. Metal–Support Interaction and Charge Distribution in Ceria-Supported Au Particles Exposed to CO. *Chem. Mater*., 34, 17, 7916–7936, 2022. DOI: 10.1021/acs.chemmater.2c01659.

A12. L. Piliai, P. Matvija, T. N. Dinhová, I. Khalakhan, T. Skála, Z. Doležal, O. Bezkrovnyi, L. Kepinski, M. Vorokhta, I. Matolínová. *In-situ* spectroscopy and microscopy insights into CO oxidation mechanism on $Au/CeO_2(111)$ model catalyst. *ACS Appl. Mater. Interfaces*, in press (published online). DOI: 10.1021/acsami.2c15792

My contribution to the selected publications

Article **A1:** participating in the preparation and NAP-XPS study of the model M/CeO_2 (Ni, Co, Cu) catalysts, helping with processing the measured XPS spectra, and reading and editing the written manuscript. All NAP-XPS experimental data were obtained during my 2-month stay at BNL by a scientific team consisting of Zongyuan Liu, Robert M. Palomino, Mykhailo Vorokhta, and David C. Grinter.

Article **A2:** participating in the preparation and NAP-XPS study of the model Ni/CeO_2 catalysts, helping with processing the measured XPS spectra, and reading and editing the written manuscript. The experimental work was carried out using the ALS synchrotron in Berkeley (USA) during a five-day experiment by a scientific team consisting of Robert M. Palomino, David C. Grinter, and Mykhailo Vorokhta.

Article **A3:** conceptualizing the experiment, designing the experimental set-up for the *in operando* NAP-XPS study of the SnO_2-based gas sensor, making NAP-XPS measurements (with the participation of Martin Vondráček), processing XPS spectra, writing the manuscript draft, submitting the manuscript to the journal and performing most of the work connected with its publication.

Article **A4:** conceptualizing the experiment, performing the *in operando* NAP-XPS study of the CuOx NWs-based gas sensor (with the participation of Pavel Hozák), processing XPS spectra, writing the manuscript draft, submitting the manuscript to the journal and performing most of the work connected with its publication.

Article **A5:** making NAP-XPS measurements (with the participation of Oleksii Bezkrovnyi), processing XPS spectra, and reading and editing the written manuscript.

Article **A6:** making NAP-XPS measurements (with the participation of Oleksii Bezkrovnyi and Piotr Kraszkiewicz), processing XPS spectra, writing the NAP-XPS part of the manuscript, and reading and editing the written manuscript.

Article **A7:** conceptualizing the experiment, performing the *in operando* NAP-XPS study of the ZnO NRs-based gas sensor (with the participation of Lesia Piliai), processing XPS spectra, writing the manuscript draft (except for the Response of Sensor in Dc- and Ac-Modes chapter written by M. Vrňata), and performing most of the work connected with its publication.

Article **A8:** conceptualizing the experiment, performing the *in operando* NAP-XPS study of the ZnO NRs-based gas sensor (with the participation of David Tomeček and Lesia Piliai), processing XPS spectra, writing half of the manuscript draft (the NAP-XPS part, Abstract, Conclusions, formatting the manuscript), submitting the manuscript to the journal and performing most of the work connected with its publication.

Article **A9:** making NAP-XPS measurements (with the participation of Frederic C. Meunier, Luis Cardenas, Helena Kaper, and Břetislav Šmíd), processing XPS spectra, and reading and editing the written manuscript.

Article **A10:** conceptualizing the experiment, performing the *in operando* NAP-XPS study of the Ru/CeO_2 catalyst (with the participation of Oleksii Bezkrovnyi and Lesia Piliai), processing XPS spectra, writing half of the manuscript draft (the NAP-XPS part), submitting the manuscript to the journal and performing most of the work connected with its publication.

Article **A11:** conceptualizing the experiment, performing the *in operando* NAP-XPS study of the model Au/CeO_2 catalyst (with the participation of Oleksii Bezkrovnyi and Lesia Piliai), performing the SRPES study of the model Au/CeO_2 catalyst (with the participation of Tomáš Skála and Ivan Khalakhan), processing XPS and SRPES spectra, writing the NAP-XPS and SRPES part of the manuscript draft, and performing a substantial amount of the work connected with its publication.

Article **A12:** conceptualizing the experiment, performing the *in operando* NAP-XPS and SRPES study of the model Au/CeO_2 catalyst (with the participation of Lesia Piliai, Tomáš Skála, and Ivan Khalakhan), processing XPS and SRPES spectra, writing the manuscript draft, submitting the manuscript to the journal and performing most of the work connected with its publication.